2 copies

NASA CR 114556

Available to the Public

PHASE 1 FINAL REPORT
VENUS WIND-ALTITUDE RADAR STUDY

by Lester I. Goldfischer

January 1973

Prepared under Contract NAS2-7255 by
THE SINGER COMPANY-KEARFOTT DIVISION
PLEASANTVILLE, N.Y.
FOR
AMES RESEARCH CENTER
NATIONAL AERONAUTICS AND SPACE ADMINISTRATION

Kearfott Doc. No. Y256E012
DRR No. 01394 (NP)
01305 (P)
00016 (P)

SINGER
AEROSPACE & MARINE SYSTEMS

SUMMARY

A three-month study of a wind/altitude radar for a Venus probe was carried out. The baseline configuration was taken to be the SKD-2100 Doppler radar modified to accommodate the altimeter portion of the APN-187 and a single beam antenna. Using current models of the Venus environment, engineering studies were made to define design requirements and to estimate the operational and physical characteristics of the conceptual design.

The results of the study are that the radar instrument would have an altitude limit of at least 34 km for velocity and at least 17.5 km for altitude measurement. Vertical velocity accuracy should be better than ±0.9% and horizontal velocity accuracy should be better than ±3% over the operating altitude range. Altimeter accuracy should be within ±3% up to about 2.5 km and should improve over the remainder of the altimeter operating range. The radar is expected to require between 48.5 and 69.3 watts of power and to weigh between 3.86 and 5.21 kg (8.5 and 11.5 lb). In each case, if power could be supplied directly from the probe batteries the lower figures would apply; the upper figures would apply if a power conditioner must be used. The electronics are expected to fit into a volume of 8200 cm^3 (500 in^3); the planar antenna would be mounted outside the probe pressure vessel in a 25.4 cm x 25.4 cm x 1.905 cm (10" x 10" x 3/4") volume. (Weight and volume estimates were made principally in terms of the English system of units.)

This work was performed by Singer-Kearfott for NASA Ames. The project monitor for the Ames Research Center was J. Sperans. At Kearfott, the program was supervised by G. Stavis and the project engineer was L. Goldfischer. Assistance in carrying out specific tasks was provided by L. Vladimir (design requirements), Dr. G. R. Gamertsfelder (engineering studies), T. Vagt (conceptual design) and E. Chin (antenna).

THE SINGER COMPANY • KEARFOTT DIVISION

REVISION RECORD

CONTROL (A)

REV	DESCRIPTION	APPROVAL AND DATE
-	Original Issue	L.A.B. 2/12/73

REV	-																				-
PAGE	COVER																				OTHER PAGES
REVISION SYMBOL OF REVISED PAGES																					
ASTERISKS (*) SHOWN LOCATE CHANGES FROM PREVIOUS ISSUE FOR CONVENIENCE ONLY - NO LIABILITY ASSUMED																					

TABLE OF CONTENTS

LIST OF FIGURES

Page No.

I. INTRODUCTION

This report describes the results of a three-month study conducted under Phase I of Contract NAS2-7255 for NASA Ames by the Kearfott Division of the Singer Company. The subject of the study was a light weight, low power radar instrument capable of measuring wind velocity and vehicle altitude during the descent of a Venus atmospheric entry probe. It was the purpose of the study to estimate the accuracy of the measurements and the useful operating range achievable by a radar instrument resulting from a low cost, minimum development effort. To meet these last constraints, the baseline configuration for all of this work was taken to be the SKD-2100 Doppler radar modified to accommodate a single beam antenna and the altimeter portion of the APN-187.

Four specific tasks were covered in the course of the investigation. The first of these was to define the design requirements of the radar instrument based on the expected descent profile of the probe, the best available knowledge of the characteristics of the atmosphere and surface of Venus, and system constraints furnished by the Ames Research Center. To meet the resultant design requirements, the next task was to generate a conceptual design based on modification of the SKD-2100 Doppler radar and the altimeter portion of the APN-187. The third task was to perform engineering studies aimed at optimizing the conceptual design with respect to the mission and system constraints, and the last task was to examine the feasibility of the selected approach. For this purpose, the accuracy and operating range were estimated as well as the overall size, weight and power needed to do the job. Each of the four tasks summarized above is described in detail, along with its results, in the sections which follow.

2. TASK DESCRIPTIONS

2.1 DEFINITION OF DESIGN REQUIREMENTS

It would be desirable for the radar instrument to be operational as soon as possible after the probe begins its free fall through the Venus atmosphere. This portion of the mission starts at an altitude of about 45 km, when the restraining parachute is jettisoned. The task of defining design requirements started by examining the expected velocity profile of the probe from 45 km down to the surface. In conjunction with the transmitter frequency and the antenna parameters, knowledge of the velocity profile is needed to determine the range of Doppler shifts and echo spectrum bandwidths which must be accommodated.

The expected variation of vertical velocity with altitude below 45 km is shown graphically in Figure 1. Two sets of data points are included, a basic set derived by measuring the tangent along a typical descent profile [1] and a set calculated from a simple analytic approximation to be used in subsequent computer studies. The range of vertical velocities runs from 53.5 m/s at the top altitude to 10 m/s at impact. Along with the vertical motion induced by the force of gravity, the probe will also experience horizontal motion as a result of wind. Although it is not possible to set forth a horizontal velocity profile, there is some evidence that wind speeds below 45 km will be less than 30 m/s, with higher velocities occurring at the upper altitudes [2].

In addition to being directly proportional to the velocity of the vehicle, the Doppler shift is also inversely proportional to the velocity of propagation in the transmission medium (i.e. the atmosphere of Venus) at the antenna interface. Because of the more than 10:1 variation in density expected over the altitude

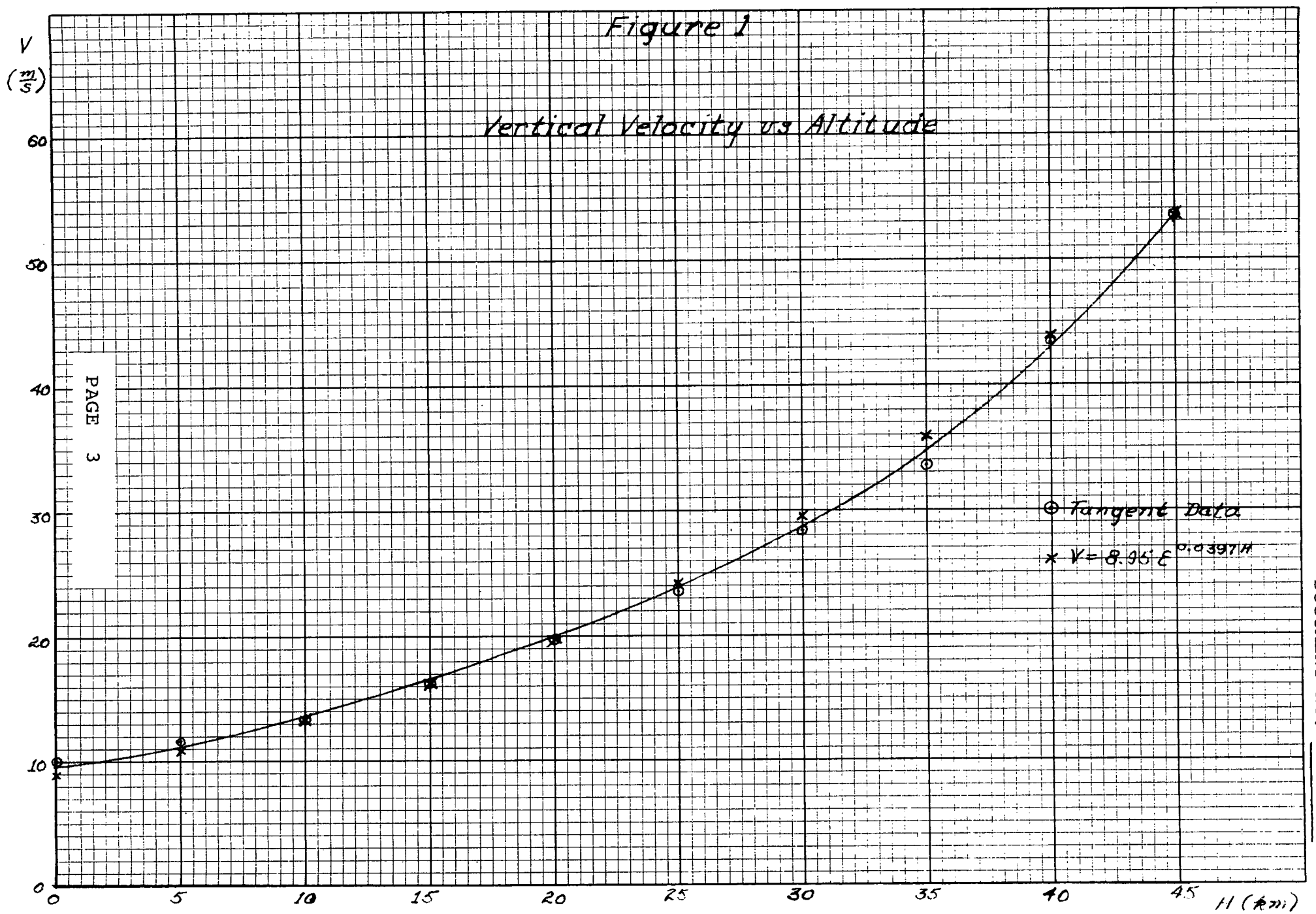

range of interest, the variation in propagation velocity with altitude is not insignificant. Use of the density vs altitude data for the most probable model of the atmosphere of Venus [3] and the Clausius-Mosotti function for CO_2 [4] permits the calculation first of ε_r, the relative dielectric constant and then of v_r, the velocity of propagation relative to a vacuum. These are plotted with respect to altitude in Figure 2. Over the altitude range of interest, the overall variation in ε_r is about 3% while the maximum change in v_r is about 1.5%.

The change in propagation velocity with altitude also affects the altimeter function since it changes the proportionality between propagation path length and round-trip delay. To calculate the change in t_r, the relative delay, as a function of altitude, v_r was approximated by a quadratic in altitude. Then the reciprocal of v_r (i.e. the relative delay per unit propagation path length) was integrated with respect to altitude between the limits (0,H) where H is the altitude of interest. Normalizing the result by H yielded t_r, which is also shown plotted against altitude in Figure 2. The overall change in t_r is about 1% over the altitude range of interest.

Atmospheric effects in the vicinity of Venus, in addition to causing changes in propagation time with altitude, are also expected to result in a large altitude and wavelength dependent loss factor. The dependence on altitude comes about by way of the large variation in pressure and temperature in the Venus atmosphere with altitude, i.e. the loss factor may be written as a function of pressure, temperature and wavelength [5]. To calculate the round-trip attenuation at any given altitude, it is necessary first to compute the loss factor (i.e. attenuation per unit path length) as a function of altitude and then find

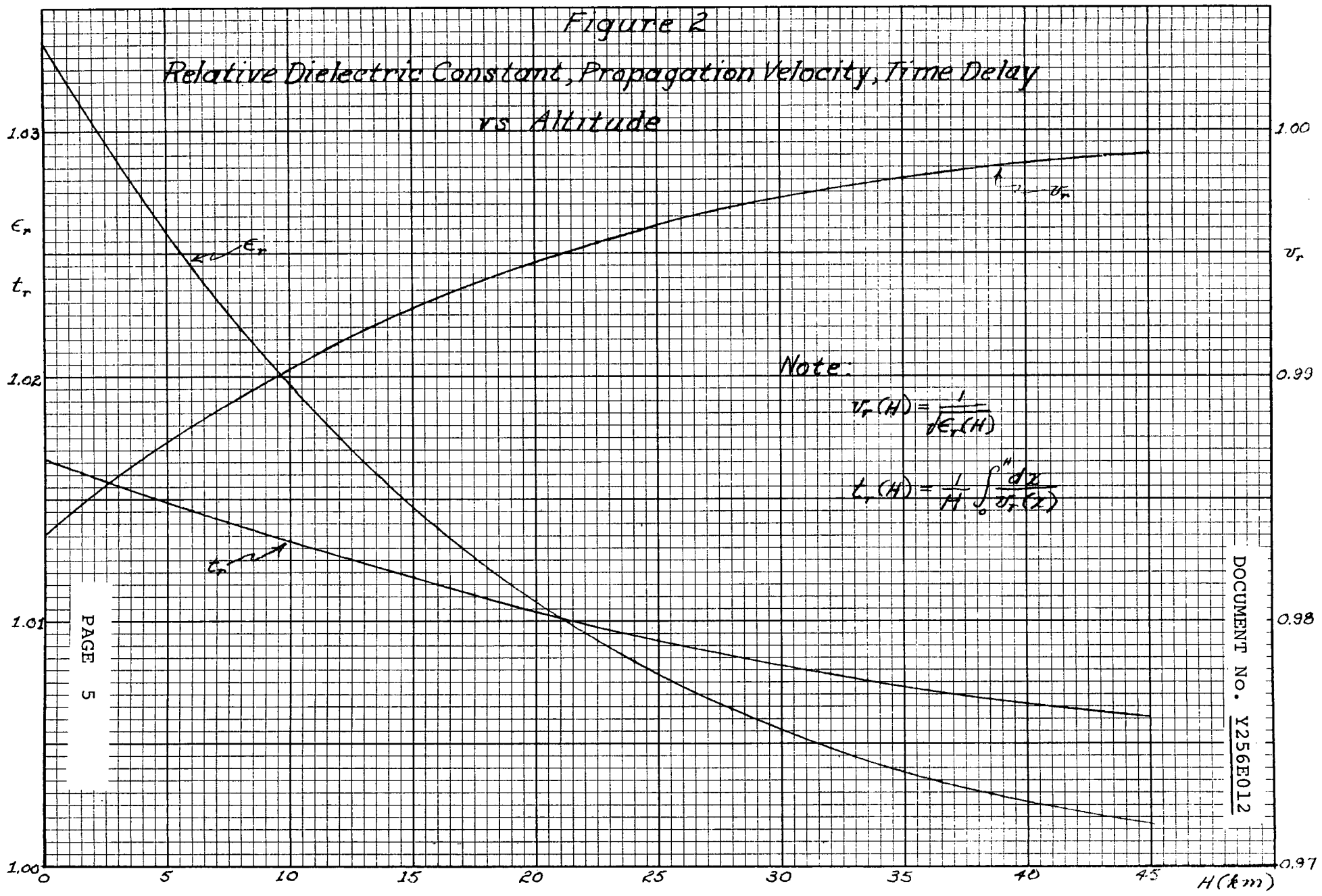

twice the integral of this function from the surface up to the altitude of interest. When these operations were carried out with λ = 2.25cm (which is the SKD-2100 transmitter wavelength) using the pressure and temperature data vs altitude for the most probable atmosphere composed of 97% CO_2 and 3% N_2 [3], the total atmospheric attenuation turned out to be 16 dB. For these calculations, the model atmosphere data was used under the assumption that the radius of Venus is 6050 km. However, when measurements of the total atmospheric attenuation [6] are extrapolated to λ = 2.25cm, they yield a value of 25 dB with a ±2 dB uncertainty. In an attempt to reconcile these two different results, a new set of calculations was made taking 6046 km as the radius of the surface of Venus (when using the tabulated model atmosphere data). This time the total calculated atmospheric attenuation was 22.5 dB, which is considered reasonably close to the measured result.

A plot of the expected round-trip atmospheric attenuation vs altitude, calculated as described in the previous paragraph, appears in Figure 3. As stated on the graph, the assumed wavelength is λ = 3cm. To determine the attenuation at any arbitrary wavelength, λ_a, the ordinates in Figure 3 should all be multiplied by $(3/\lambda_a)^2$. The reason for using λ = 3cm as the basis for this plot is that the SKD-2100 can be made to operate at that wavelength without major changes and, more important, the maximum atmospheric attenuation drops to 12.7 dB. For consistency, all further calculations reported here which are wavelength dependent will assume λ = 3cm. A simple approximation to the loss curve suitable for computer studies is also shown in Figure 3. Before leaving this subject, it should be mentioned that there is Mariner 5 data for altitudes above 34 km [7] which indicate even higher attenuation than shown in Figure 3. However, subsequent developments in this study show that this is outside the useful

twice the integral of this function from the surface up to the altitude of interest. When these operations were carried out with λ = 2.25cm (which is the SKD-2100 transmitter wavelength) using the pressure and temperature data vs altitude for the most probable atmosphere composed of 97% CO_2 and 3% N_2 [3], the total atmospheric attenuation turned out to be 16 dB. For these calculations, the model atmosphere data was used under the assumption that the radius of Venus is 6050 km. However, when measurements of the total atmospheric attenuation [6] are extrapolated to λ = 2.25cm, they yield a value of 25 dB with a ±2 dB uncertainty. In an attempt to reconcile these two different results, a new set of calculations was made taking 6046 km as the radius of the surface of Venus (when using the tabulated model atmosphere data). This time the total calculated atmospheric attenuation was 22.5 dB, which is considered reasonably close to the measured result.

A plot of the expected round-trip atmospheric attenuation vs altitude, calculated as described in the previous paragraph, appears in Figure 3. As stated on the graph, the assumed wavelength is λ = 3cm. To determine the attenuation at any arbitrary wavelength, λ_a, the ordinates in Figure 3 should all be multiplied by $(3/\lambda_a)^2$. The reason for using λ = 3cm as the basis for this plot is that the SKD-2100 can be made to operate at that wavelength without major changes and, more important, the maximum atmospheric attenuation drops to 12.7 dB. For consistency, all further calculations reported here which are wavelength dependent will assume λ = 3cm. A simple approximation to the loss curve suitable for computer studies is also shown in Figure 3. Before leaving this subject, it should be mentioned that there is Mariner 5 data for altitudes above 34 km [7] which indicate even higher attenuation than shown in Figure 3. However, subsequent developments in this study show that this is outside the useful

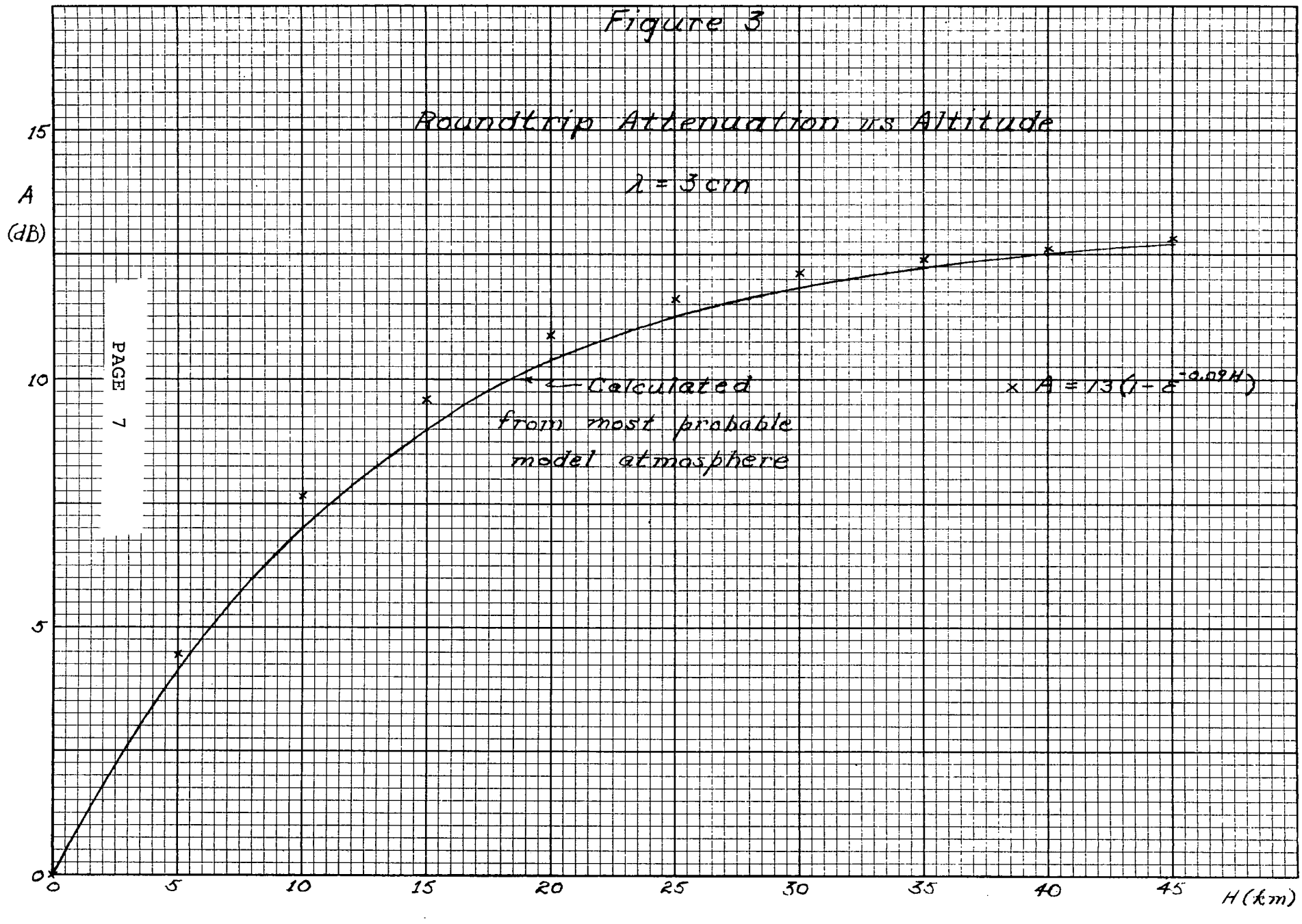

operating range of an instrument meeting the constraints of the program.

On top of the atmospheric loss just discussed is an additional loss expected to occur upon backscattering from the surface of Venus. At normal incidence, the reflectivity of the surface is generally accepted to be about 15% [6]. Departing from the normal by 10°, at λ = 3.8cm, the reflectivity is down about 8 db with a negative slope in that vicinity of about 1 dB/degree [8]. For λ = 3cm and incidence angle of 10° from the vertical, the use of 16 dB as the total backscattering loss should be conservative. Furthermore, setting the design center of the radar beam to be 10° from the vertical as the probe vehicle descends is considered to be a reasonable compromise between holding down transmission path and backscattering losses while maintaining sensitivity to horizontal velocity components. Although the losses would be absolutely minimized with a vertical beam, there would also be absolutely no Doppler shift in the presence of horizontal velocity.

The two kinds of atmospheric effects discussed so far, i.e. variation in propagation velocity and losses with altitude, give rise to two sets of design requirements on the radar instrument. First, the antenna must be designed in such a way as to minimize variations in velocity calibration constant associated with propagation velocity changes. Since the antenna must be outside the pressure vessel, it must also be designed to withstand the high temperature and pressure expected near the surface of Venus. In the next section, an antenna design aimed at meeting these requirements is described. The large atmospheric losses, and the desirability of high altitude operation (45 km as compared to 3 km specified for the SKD-2100 operating over Earth) generates a requirement for an increase in transmitter power. Part of the increase is achieved, in effect, by going from a switched beam

arrangement (in the standard SKD-2100) to a single beam arrangement; a reduction of 9.5 dB in front end losses is accomplished this way. The remainder of the increase is achieved by using a higher power transmitter source; studies of the SKD-2100 showed that it is perfectly feasible to replace the 50 mW solid state source used in the standard unit with a 0.5W solid state source, the latter being within the means of available technology. Engineering studies of the radar instrument, found in Section 2.3, use the 0.5W source as the basis of computation.

Operation at high altitude creates another design requirement not imposed on the standard SKD-2100. In an FMCW system using sinusoidal modulation, the beat note between the echo and the transmitter is generally also sinusoidally frequency modulated. The useful signal in the SKD-2100 is a first order sideband of the beat note. However, when the round trip delay of the echo is one period of the FM wave, the beat note is not modulated and the useful signal disappears. For the 30 kHz modulation frequency used in the SKD-2100 and a beam squint angle of 10°, this occurs at an altitude of 5 km and multiples thereof. At such altitudes and their immediate neighborhoods, the radar is said to be in an altitude hole. To overcome that difficulty here, it is intended to use two FM frequencies, 30 kHz and 33 kHz, alternately for equal time intervals at a 4.8 Hz rate and to average over the two regimes. The details of this modification are described in the next section.

The use of two FM frequencies also fits the requirements of the altimeter portion of the APN-187. As a consequence of the two frequencies chosen (and to the extent that adequate signal-to-noise ratio is available) it should be possible to determine altitude unambiguously halfway up to the common hole, viz. 25 km. Another (back-up) mode for altitude determination

will be available upon processing the received data. This is by integrating vertical velocity, using the low altitude altimeter output (where an adequate signal-to-noise ratio is reasonably certain) to establish the constant of integration.

The single beam antenna of the radar instrument is required to be compatible with the 55.9 cm (22 inch) diameter spherical pressure vessel which constitutes the probe vehicle during the descent through the lower atmosphere. To meet this requirement, the antenna configurations studied were limited to a 25.4 cm x 25.4 cm (10" x 10") projected aperture. Plane or cylindrical versions would be mounted symmetrically with respect to the spin axis; it is expected that under these conditions, only minor aerodynamic effects would be experienced. At a wavelength of λ = 3cm, the one-way beamwidth would be about 6° which is only 10% greater than on the standard SKD-2100. Another requirement on the antenna is that it not impede viewing out along the spin axis through a 2.54 cm x 2.54 cm (1" x 1") aperture. Studies made on the basis that the antenna would consist of two sections separated by a 2.54 cm (1 inch) slot showed that the principle effect at λ = 3cm would be to limit sidelobe reduction in planes normal to the slot to 11 dB one way. This is not considered to be a significant limitation on the design. (In the course of the calculations reported in this paragraph, English units were used for the dimensions of both the antenna and the spherical pressure vessel.)

Rotation of the radar beam around the spin axis, which is assumed to be vertical, means that the Doppler shift associated with the horizontal component of velocity will be cyclic at the spin rate. The vertical component of velocity on the other hand will give rise to a steady component of Doppler shift. Separation of the two components of velocity would be done best by means of synchronous detection locked to the spin rate; keying the synchronous detector at any frequency within 5% of the spin rate would

also be usable but the results would require more interpretation. The requirement that output be transmitted every kilometer at the top of the altitude range translates into a rate of about (1 sample)/(20 seconds). Given a spin rate of 10-15 rpm, this permits averaging over four spin cycles before each transmission. How all this would be implemented is described in the next section.

2.2 CONCEPTUAL DESIGN

The basic configuration of the velocity/altitude radar instrument consists of the SKD-2100 Doppler system modified to work with the altimeter portion of the APN-187 and a single beam antenna. A block diagram showing the salient features of the radar instrument appears in Figure 4. The antenna, stripline front end, pre IF, timer and buffer/interface are shared by both velocity and altitude channels. Each of the channels has its own post IF, one leading to the frequency tracker in the velocity channel and the other to the phase-splitter, doubler, filter, mixer and phase-locked loops of the altitude channel.

Almost the entire radar instrument is derived, either on a module or on a circuit basis, from the SKD-2100 and the altimeter of the APN-187, principally the former. The stripline assembly would be taken intact from the SKD-2100. In the case of the pre IF assembly, the existing module in the SKD-2100 would be modified by the addition of the amplifier, filter and driver amplifier group shown as providing a J_1 Doppler double side band signal for the altitude channel. This last group, however, would use the same circuit designs now used for the corresponding group in the SKD-2100, i.e. the same as the group which furnishes the J_1 Doppler single sideband signal for the velocity channel.

FOLDOUT FRAME 1

FOLDOUT FRAME 2

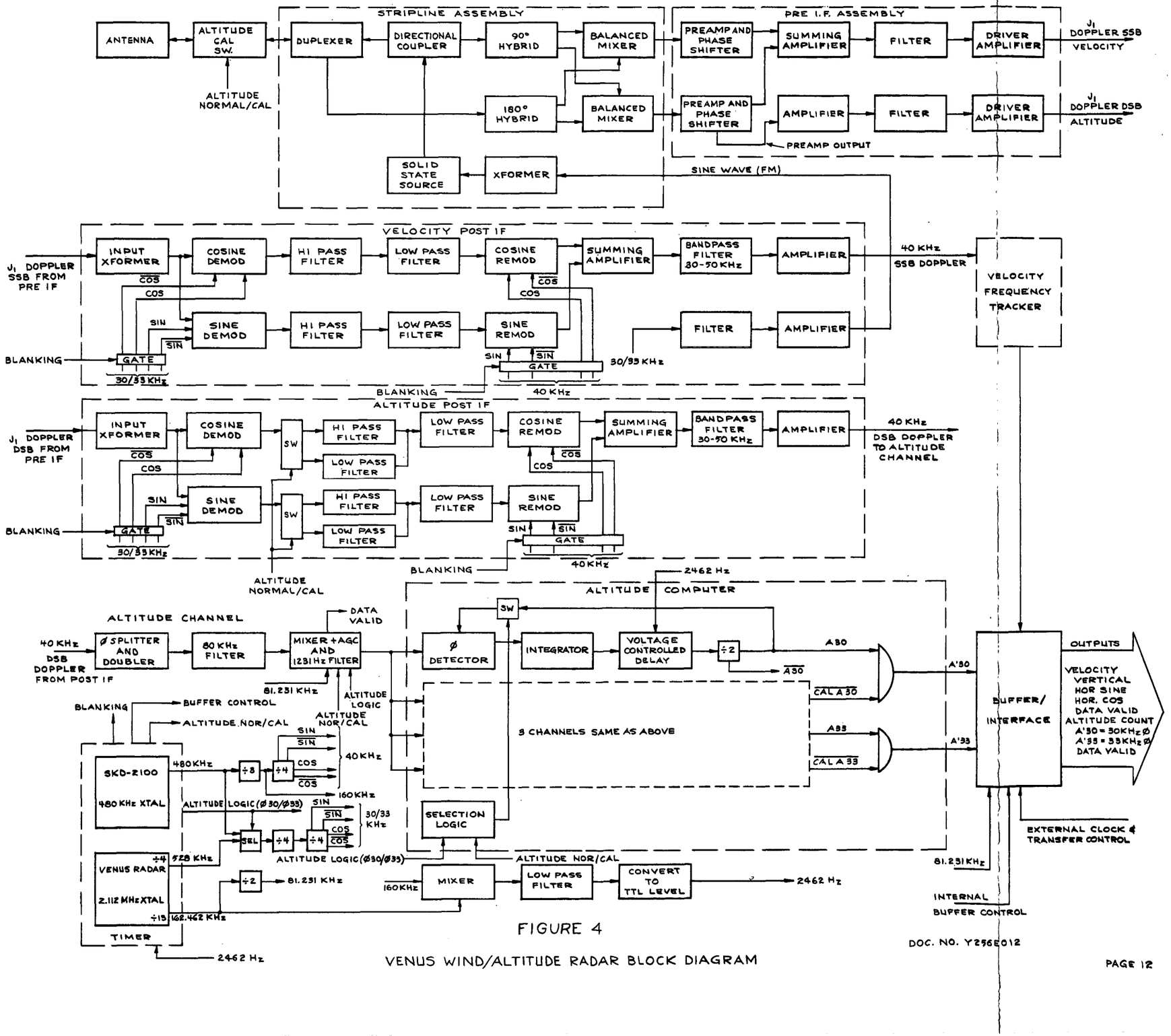

FIGURE 4

VENUS WIND/ALTITUDE RADAR BLOCK DIAGRAM

Each of the post IF modules in the Venus probe radar would be essentially a duplicate of the single post IF found in the SKD-2100 but with the time sharing switches (needed for multibeam operation in the SKD-2100) disabled. Two additional modifications would be made for the altitude post IF: the filter and amplifier used (in the velocity post IF) to create the FM drive signal would be eliminated and the time sharing switches would be adapted for the altitude normal/calibrate function. The purpose of this function will be described subsequently. Also taken essentially intact from the SKD-2100 would be the frequency tracker; the only modification needed here is, again, the disabling or elimination of time sharing switches. In a similar fashion, the entire altitude channel, including the phase splitter, 80 kHz filter, mixer and the four phase tracking loops which make up the altitude computer would be taken intact from the APN-187 with only minor changes in some frequency selective circuits.

The timer and its associated divider chains and mixer group (producing 40 kHz, 30/33 kHz and 2462 Hz) would be a new unit although it would include part of the SKD-2100 timer. The antenna, altitude calibrate switch and buffer/interface units would be entirely new, implementing designs created specifically for the Venus wind/altitude radar.

The signal transmitted from the antenna is an FMCW wave sinusoidally modulated at either 30 kHz or 33 kHz, alternation between the two frequencies occurring at 4.8 Hz with a 50% duty ratio. As a result of homodyne detection in the stripline front end, the output of the two balanced mixers contain echo spectra symmetrically positioned around each of the harmonics of the transmitted modulation frequency. Because of the 90° hybrid which precedes the two mixers and the subsequent use of phase

shifters (which maintain a broadband 90° relative phase difference near the modulation frequency) the output of the summing amplifier contains only the upper sideband echo spectra. The filter which follows passes only the sideband closest to the modulation frequency; this is denoted "J_1 Doppler SSB, Velocity" in Figure 4. For the altitude channel, the single sideband summing operation is avoided and the equivalent filter passes only the two sidebands closest to (and symmetrically displaced from) the modulation frequency; this is denoted "J_1 Doppler DSB, Altitude" in Figure 4.

In principle, an FMCW system operating around the J_1 sideband should provide infinite discrimination against antenna or front end reflections. However, the real world rarely behaves exactly like its mathematical models and this is no exception. A small amount of reflection leakage is always present right at and near the fundamental modulation frequency. It is the function of the post IF to remove the leakage term so that it cannot saturate higher gain stages or cause other difficulties. This is accomplished by referencing the signal to zero frequency in two quadrature channels by mixing with the modulation frequency, high pass filtering to remove the leakage (now at and near zero frequency) then remodulating in quadrature at 40 kHz and summing. As a result of the last step, the echo spectrum is referenced to 40 kHz (i.e. displaced from 40 kHz by the Doppler shift) and the FM switching has been removed. Blanking is applied to the demodulation and remodulation keying signals to avoid transient disturbances around the instants when transition is made between 30 to 33 kHz. Since the round trip delay time at the maximum altitude would be 300 μs, a blanking interval of about 0.8 ms would be used.

The process of leakage elimination just described is reversed periodically for calibration purposes in the altitude post IF. Once every fourth spin cycle, with an overall duty ratio of 1:16, the altitude normal/calibrate switch (between the antenna and duplexer) would be activated, deliberately creating a small but controlled reflection. Simultaneously, switching after the demodulators in the altitude post IF would select low pass (instead of high pass) filters, capturing the leakage calibration signal and eliminating the normal Doppler signal. At the same time, additional switching in the altitude computer would select the 30 kHz and 33 kHz calibration phase tracking loops so that the phase shift associated with zero altitude could be established for each of these frequencies.

During normal altitude computation, the symmetrical Doppler sidebands, each displaced from 40 kHz are brought into a phase splitter followed by a full wave linear detector acting as a doubler. Here the second harmonic of the previously suppressed carrier is recreated. It is the phase of this 80 kHz signal which carries the altitude information. After filtering, this signal is mixed down to 1231 Hz (with, at most, a constant displacement of phase) and processed in one of the two normal phase tracking loops, the choice depending on whether 30 kHz is active or 33 kHz. The outputs of the normal phase tracking loops are 50% duty ratio square waves at 1231 Hz denoted by A30 and A33 in Figure 4. Combining each of these with the opposite phase of the corresponding calibration loop in a logical AND circuit (e.g. $A30 \cdot \overline{CAL\ A30}$) results in two gate waveforms at 1231 Hz.

Denoting the gate associated with the use of 30 kHz FM by A'30 and that associated with the use of 33 kHz FM by A'33, the width of the active portion of the gate in each case turns out to be a symmetrical sawtooth function of altitude. Starting at a given altitude hole, in each case the gate width rises linearly with altitude to a maximum of 1/2462 second at a point midway between altitude holes and then subsides linearly, reaching zero at the next altitude hole. To put all of this in perspective, altitude holes occur at multiples of 5.08 km for 30 kHz FM and at multiples of 4.62 km for 33 kHz. When the system is in a hole at either FM rate and the signal-to-noise ratio is insufficient for useful operation, indication is made through loss of the DATA VALID signal. As a result of the choice of 30 kHz and 33 kHz, simultaneous loss of signal due to altitude hole effects cannot occur anywhere within the desired altitude range.

The generation of the FM rate switching waveforms would be carried out as indicated by the upper portion of the block diagram which appears in Figure 5. Alternate selection of 30 kHz and 33 kHz FM rates for equal intervals at a 4.81 Hz rate would be accomplished by a counter chain dividing the 2462 Hz input by 256. (Generation of the 2462 Hz signal is shown at the bottom of Figure 4.) Creation of the post IF blanking pulse (to prevent transients when switching between 30 kHz and 33 kHz) is also shown at the top of Figure 5. The duration of the blanking pulse would be 1/1231 second and it would be timed to straddle each FM rate transition. Formation of the pulse trains needed for the readout of velocity would be accomplished in the manner indicated by the lower portion of the block diagram in Figure 5. The velocity sampling rate indicated here is 0.801 Hz and presumes that the vehicle spin rate is within 5% of 12 rpm, making about 4 samples per spin cycle. Each sample would have a duration of 1/1231 second. At the bottom of Figure 5 is shown the creation of

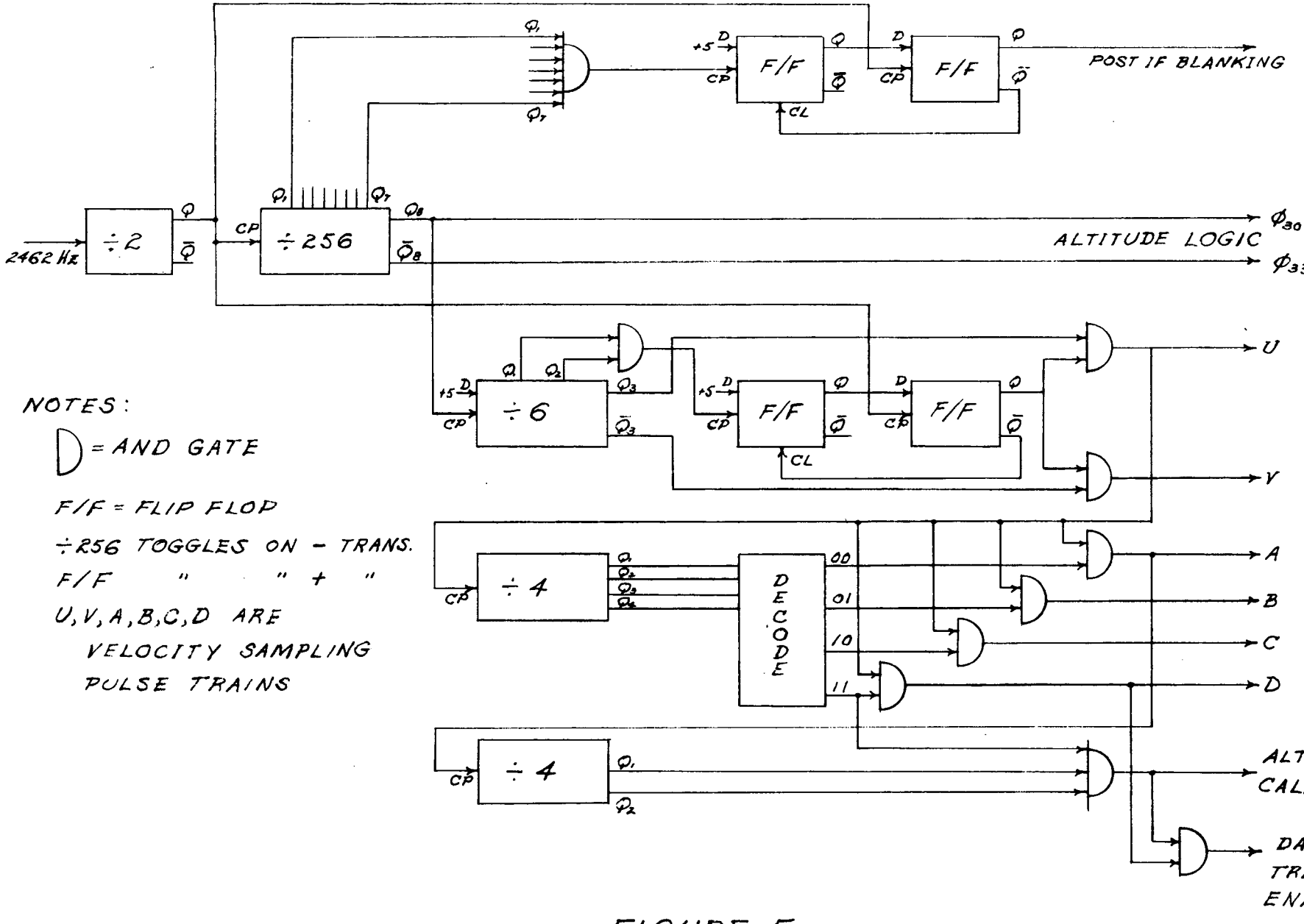

FIGURE 5

SWITCHING/SAMPLING TIMER BLOCK DIAGRAM

the altitude calibrate and data transfer enable signals.

Altitude readout would be accomplished as indicated by the block diagram which appears in Figure 6. Two quantities must be reported, one proportional to the round trip phase delay when 33 kHz is the FM rate and the other proportional to the phase delay when 30 kHz is the FM rate. In each case, the sense of the block diagram is that the indicated phase delay for one FM frequency is sampled after its associated phase tracking loop has been opened. Thus $A'30$, whose ON time is cyclicly related to the phase delay at 30 kHz, gates 81.231 kHz pulses into the (30) counter during the ON time of $\phi 33$, i.e. when a phase-tracking loop associated with 33 kHz is active. The double flip-flop loop acts to select just one ON interval of $A'30$ during the ON time of $\phi 33$. ($A'30$ can be ON for at most 1/2462 second while $\phi 33$ is ON for 1/9.62 second.) Each counter would accumulate for an interval of about 4 spin cycles after which its count would be transferred to its associated buffer. Then both counters would be cleared and the accumulation process would start again.

A block diagram showing how velocity readout would be accomplished appears in Figure 7. The Doppler shift, as reported by a quadrupled version of the frequency tracker LO, would be sampled approximately four times per spin cycle by means of the pulse trains U, A, B, C, D. Four times the tracker offset frequency, viz. 160 kHz would be sampled by the V pulse train, which exactly interleaves the U train. The widths of all of these pulses would be 1/1231 second. (Creation of the velocity sampling pulse trains is shown in the lower half of Figure 5.) Vertical velocity would be derived by counting up at the quadrupled frequency tracker LO rate during every U sampling pulse and counting down (i.e. subtracting) at the 160 kHz rate during

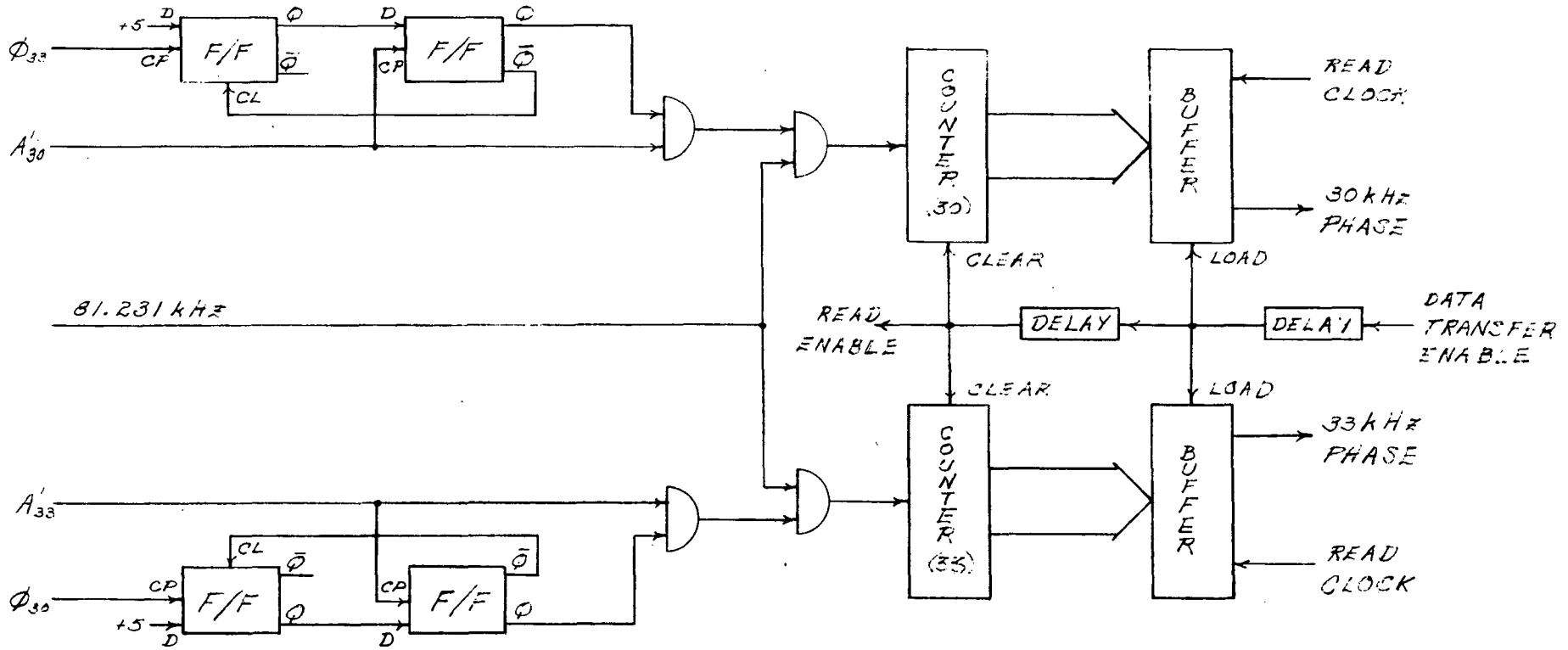

FIGURE 6

ALTITUDE READOUT SCHEME

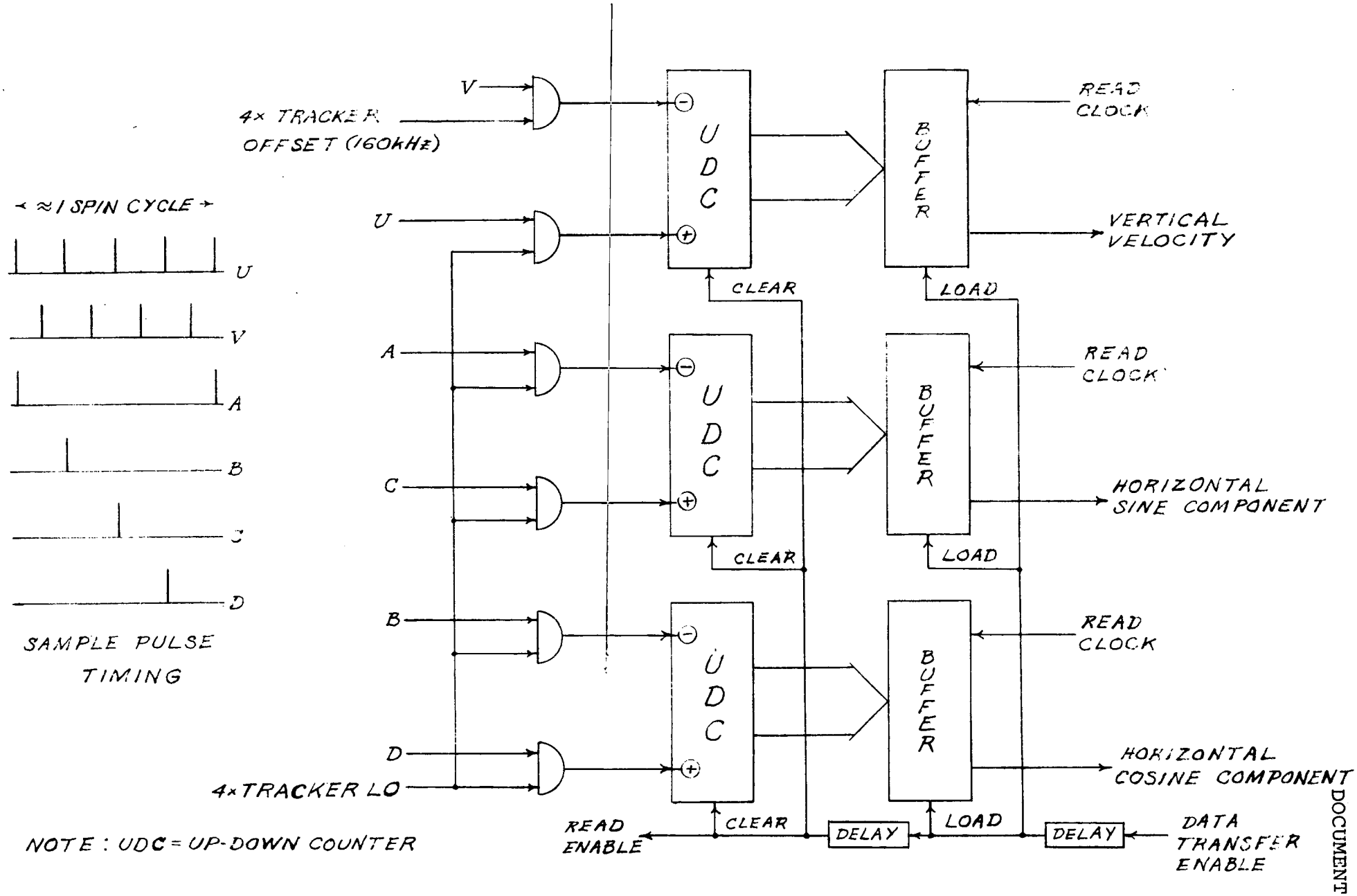

FIGURE 7

VELOCITY READOUT SCHEME

every V sampling pulse. Horizontal velocity components would be derived by counting only the quadrupled frequency tracker LO, counting up (in separate up-down counters) during the C and D sampling pulses and down (respectively) during the A and B sampling pulses. As shown in Figure 7, timing of the A, B, C and D pulse trains would be such as to make the up-down counters associated with A,C and B,D respectively the equivalent of quadrature synchronous detectors with post detection integration. After each group of 16 U or V pulses (i.e. about 4 spin cycles) the count in each up-down counter would be transferred to its associated buffer, the counters would all be cleared and the process would be repeated.

Details of the Buffer/Interface module shown at the lower right in Figure 4 have been presented in terms of the block diagrams of Figures 6 and 7. As a matter of convenience, the generation of LOAD and CLEAR (READ ENABLE) commands from the DATA TRANSFER ENABLE command is shown separately, i.e. in duplicate, in Figures 6 and 7. These commands would be generated in common for both velocity and altitude readouts in the actual Venus probe radar. Thus, the activation of the READ ENABLE line would be a signal to transmit the read clock to the various buffers in turn and effect serial readout of all output quantities.

It has been assumed here that the velocity sampling rate is not locked to the spin rate. As a result, although the root-sum-square of the sine and cosine components of horizontal velocity is clearly the magnitude of that quantity, to establish its direction requires more information. The arctangent of the ratio of the sine to the cosine component of horizontal velocity (taking into account the sign of each component separately for quadrant placement) yields the phase angle of the horizontal velocity vector relative to the sampling reference. To convert

this into directional information, it is necessary to know where the probe is facing when the sampling reference (e.g. the A pulse train) occurs. If a directional reference pulse could be generated (e.g. when the horizontal projection of the radar beam points to Venus geographic north) it could be used to start a gate which could be terminated by the next A pulse. Counting a fixed frequency oscillator, both for the duration of the gate and for the interval between successive directional reference pulses, and then taking the ratio of these two numbers would yield the direction at the time when the A pulses occur. By extension, the direction of the horizontal velocity vector could be determined. Since the direction at which the A pulses occur would change with time when the sampling and spin rates are asynchronous, the procedure just described would have to be implemented continuously and the (averaged) results reported with each data transmission.

The antenna would be a planar waveguide array with a square aperture whose dimensions would be 25.4 cm x 25.4 cm (10" x 10"). (Curved arrays were considered also; the reasons for choosing a planar array are discussed in Section 2.4.) A sketch of the waveguide configuration appears in Figure 8. Individual radiating guides would have edge-cut slots arranged in anti-phase linear array format. The group of waveguides fed from the left would be designed to produce a beam deflected by 80° from the direction of propagation in those guides. At the same time, the group fed from the right would be designed to produce a beam deflected by 110° from their propagation direction. Nominally the two beams would coincide but, even more important, changes in guide wavelength and slot spacing would cause the two to move oppositely so that, although the composite beam would tend to broaden, its centroid would tend to remain fixed. (In the course of defining the antenna aperture above, English units were used for the antenna dimensions.)

NOTE: ARROW SHOW DIRECTION OF GUIDE PROPAGATION
FEED GUIDES AT SIDES, RADIATING GUIDES AT CENTER

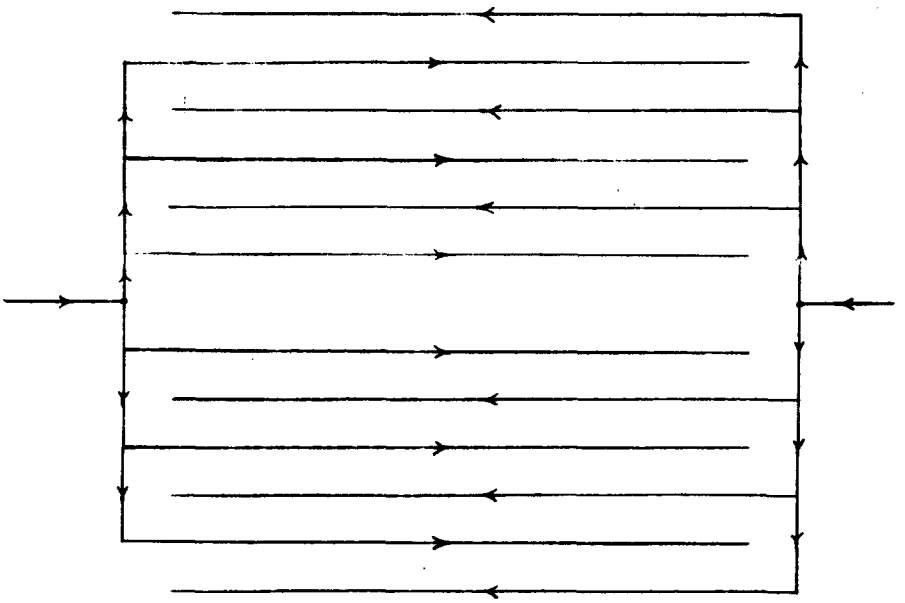

FIGURE 8

ANTENNA CONFIGURATION

Using the configuration of Figure 8, the antenna would be constructed of titanium waveguide (for dimensional stability) flashed with silver (to enhance surface conductivity) and vented to the atmosphere of Venus. The feed guides would be center fed anti-phase arrays designed to locate the radiated beam in a plane normal to the direction of feed guide propagation (i.e. broadside to the feed guides). To the extent that design symmetry can be maintained during operation, no change in this component of beam direction should occur over the altitude range of interest.

2.3 ENGINEERING STUDIES

Analysis of the radar instrument, as a whole and in part, was undertaken to provide estimates of performance and, where possible, to permit optimization of the conceptual design. In the case of the antenna, two curved configurations were considered as well as the planar configuration described in the preceding section. The first of these was a cylindrical array with a projected aperture of 25.4 cm x 25.4 cm (10" x 10"), adapted from the configuration of Figure 8 by using feed guides curved to a radius of 33 cm (13 inches). (This number was chosen to allow for 5.08 cm [2 inches] of insulation outside the pressure vessel, with the antenna up against the insulation.) It turned out that, in order to achieve a beam broadside to the feed guides, it would be necessary to terminate each of these in the center and have a separate input port at each end. Furthermore, the cylindrical array would radiate two secondary beams at ±45° from the main beam, each of which would account for 1/4 of the total input power. Although it is most likely that the system could be made to discriminate against the echo power associated with these secondary beams, the loss of half of the input power would be intollerable. By the same token, a spherical array with a 25.4 cm x 25.4 cm (10" x 10") projected aperture could be expected

to have even less acceptable losses since it would radiate four secondary beams in addition to the desired beam, the latter containing only 25% of the power input to the antenna. Thus, with respect to antenna efficiency, the planar array is clearly superior to either curved array considered.

There are several ways in which the overlapping, dual beam arrangement of Figure 8 might be carried out. On the one hand, it would be possible to use the same slot spacing but different size waveguides for the two sets of radiating guides shown in Figure 8; on the other hand, both sets could have the same size guide but with a different slot spacing in each set. Computer studies indicated that the latter alternative yielded more nearly complete compensation over the full altitude range of interest. Several different waveguide sizes were examined and, as a result of computer based comparisons, waveguide ID of 1.836 cm x 1.016 cm (0.722" x 0.400") were found to be close to optimum. Principal plane patterns were computed as a function of altitude for the following conditions:

Waveguide ID - 1.836 cm x 1.016 cm (0.722" x 0.400") @0°C,
Slot spacings - 1.999 cm (0.786") and 3.72 cm (1.463") @0°C,
Free Space Wavelength - 3 cm.

The coefficient of thermal expansion of titanium (for the waveguides) was taken to be 8.5×10^{-6} cm/cm/°C and the temperature vs altitude data was taken from a table describing the most probable atmosphere of Venus [3]. Calculation of the wavelength at the antenna interface, λ_ε, was accomplished from the relationship

$$\lambda_\varepsilon = \lambda v_r \quad ,$$

where λ is the free space wavelength and v_r is the velocity of propagation relative to a vacuum as found in Figure 2, where

it is plotted as a function of altitude. Graphs showing the variation of beam angle, measured from the normal to the array and denoted by ψ, and the (one way) beam width as functions of altitude appear in Figure 9. Most of the variation of both quantities occurs in the altitude range 0 to 15 km. Since the increase in beamwidth occurs with decreasing altitude, its effect (loss of signal-to-noise density ratio) should be quite tolerable.

Vertical and horizontal Doppler calibration constants are proportional to $(\cos\psi)/\lambda v_r$ and $(\sin\psi)/\lambda v_r$ respectively. Since λ is a constant, graphs of $(\cos\psi)/v_r$ and $(\sin\psi)/v_r$ may be used to show the variation of the two calibration constants vs altitude ascribable to the antenna. Such graphs appear in Figure 10. The change in vertical calibration constant amounts to about 1.5% overall and is attributable entirely to the behavior of v_r. The change in horizontal calibration constant is about 1.3% overall and results from opposing tendencies in $\sin\psi$ as compared to v_r. Not surprisingly, most of the change in each calibration constant occurs in the altitude range from 15 km down to the surface. (English units were used for the antenna dimensions in the calculations whose results are described in the last three paragraphs.)

The altitude limit for either function of the radar instrument is reached when the signal-to-noise ratio is insufficient to permit reliable operation of the tracking loop associated with that function. With regard to the velocity measuring function, current experience with the SKD-2100 indicates that a signal-to-noise density ratio of 6 dB at the peak of the echo spectrum is needed for proper operation of the frequency tracker. To make a preliminary determination of the maximum operating altitude for velocity measurement, the variation of peak signal-to-noise density (S/N) with altitude was calculated from the formula

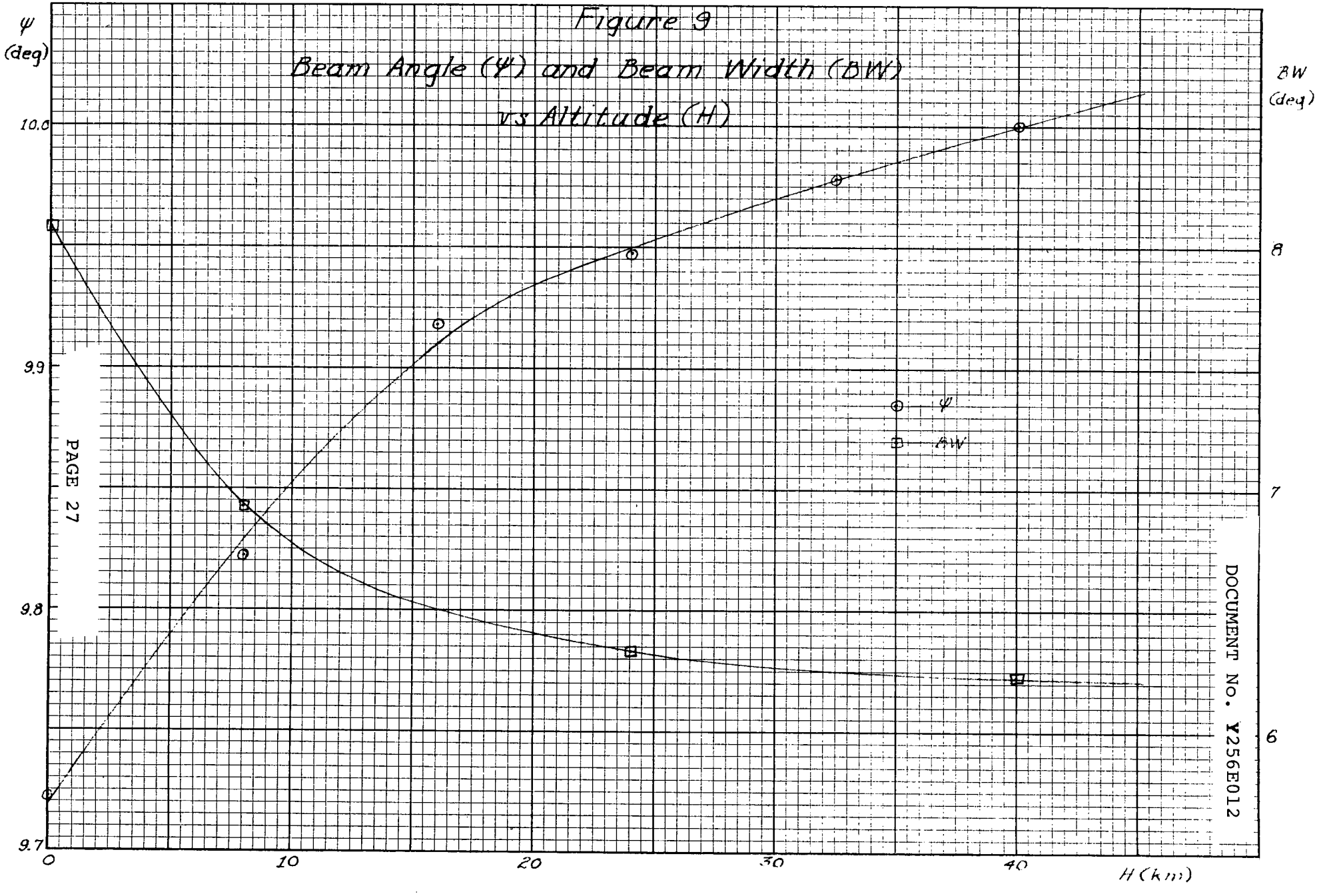

Figure 10

Calibration Constant vs Altitude

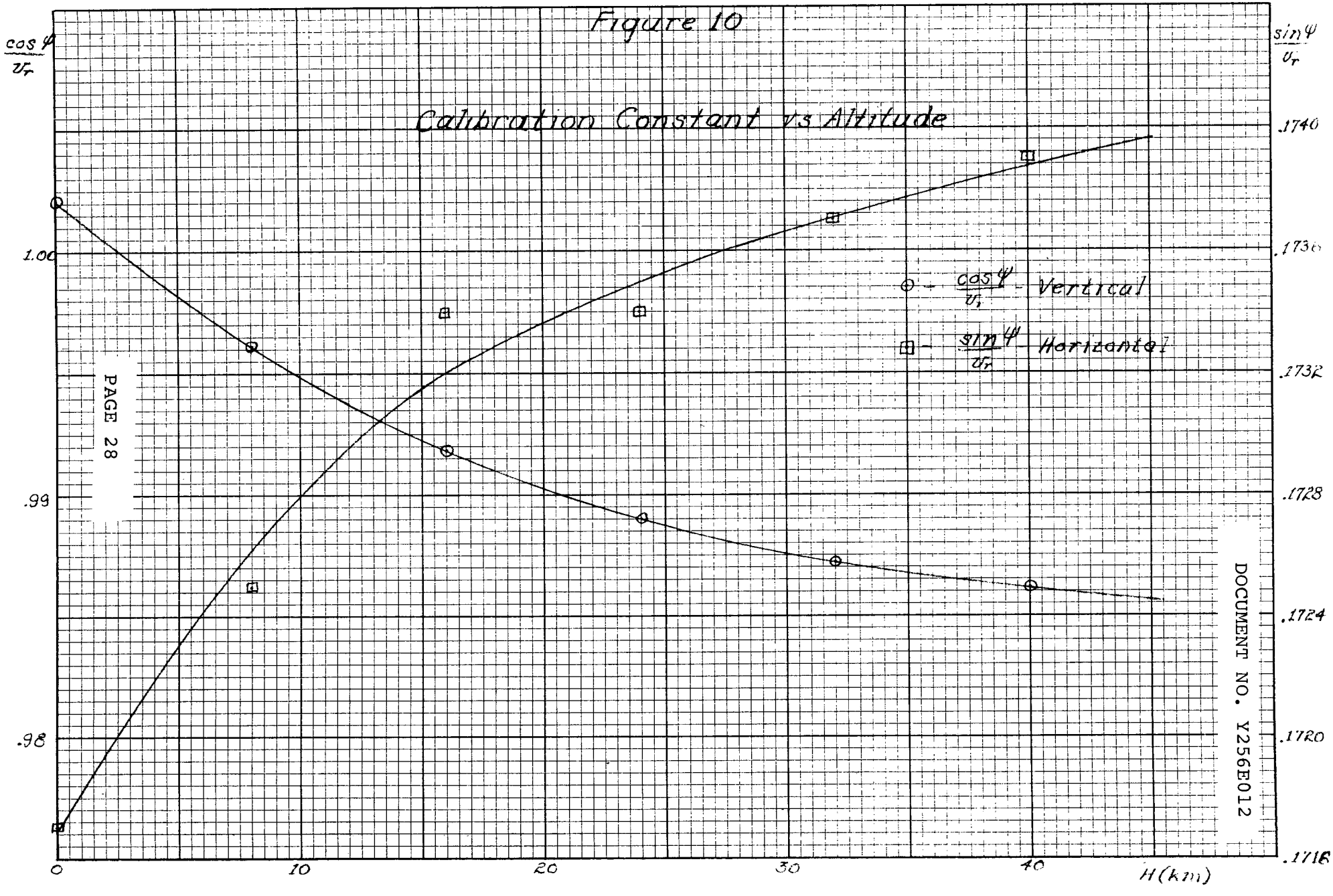

$$\frac{S}{N} = \frac{P_t \lambda^2 Gw \cos\psi \ \sigma_o L_s L_a}{16 \ \pi^2 H^2 (NF) KTB}$$

The values or defining equations for the various terms are as follows:

P_t	(transmitted power)	=	0.5W,
λ	(wavelength)	=	3×10^{-5} km,
G	(antenna gain)	=	696,
w	(pattern factor)	=	0.5,
ψ	(beam angle)	=	10°,
σ_o	(reflectivity)	=	0.02512,
L_s	(fixed losses)	=	0.1173,
L_a	(atmospheric loss)	=	$10^{-1.3}$ (1-exp[-0.09H] ,
NF	(noise figure)	=	31.62,
KT	(thermal noise)	=	4×10^{-21}W/Hz,
B	(spectrum bandwidth)	=	2 V $\sin\psi(\Delta\psi)/\lambda$,
$\Delta\psi$	(two way beamwidth)	=	$6.23\pi/180\sqrt{2}$ radians,
V	(vertical velocity)	=	$8.95 \times 10^{-3}\exp(0.0397H)$km/s.

The equations for atmospheric loss (L_a) and vertical velocity (V) are the analytic approximations given in Figures 3 and 1 respectively. Altitude (H) must be in kilometers when using these equations.

The beam angle and one way beam width were taken from Figure 9 for an altitude of 40 km. Using the selected value of beamwidth (BW) the antenna gain was calculated from the formula

$$G = \frac{27{,}000}{(BW)^2} = \frac{27{,}000}{6.23^2} \quad ,$$

which applies in the circular beam case under consideration here. The pattern factor, w, accounts for the non-uniform illumination of the surface within the main beam of the receiving pattern. For reflectivity, the value given accounts both for the intrinsic backscattering property of the surface as well as the fall off with non-vertical incidence [8]. Fixed losses include both estimated RF transmission losses in the front end and average losses associated with the FM process. The noise figure value given accounts for transmitting oscillator AM noise as well as mixer performance. Thermal noise was calculated for a temperature of 290°K, which is consistent with the controlled environment inside the pressure vessel. Since this was only a preliminary calculation of S/N, only vertical velocity was used. The results of applying the formula for S/N over a range of altitudes are summarized in the graph of Figure 11. Based on a 6 dB minimum value of S/N required for proper tracker operation, the curve in Figure 11 would indicate an upper altitude limit well above the desired operating range. However, when altitude hole effects and horizontal velocity are taken into account, as in succeeding figures, a more exact and realistic appraisal emerges.

In order to make a more exact calculation, the one way beam pattern was approximated by the equation

$$G_n = \exp(-252\theta^2) ,$$

Where G_n is the antenna pattern function and θ is the angle (in radians) from a line making an angle of 10° from the vertical. The model beam has circular symmetry and a beamwidth of just over 6° across the half power points. To keep the computation reasonable in size, for values of $\theta > 0.135$ (where $G_n < 0.01$) the pattern was assumed to be zero. The modulation

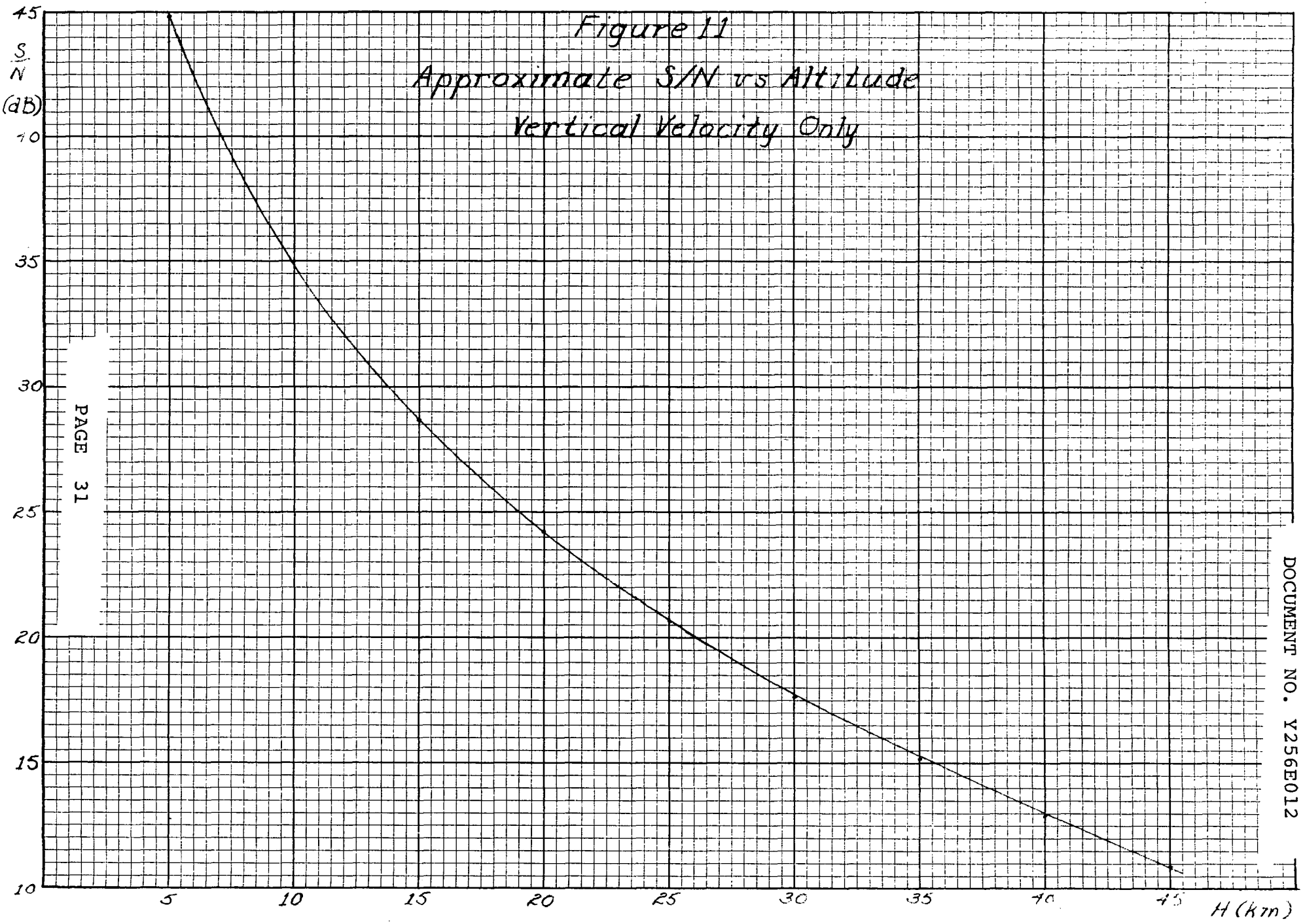

index for the transmitter was taken to be m=1 and the argument of the first order Bessel function required, denoted by a, was taken to be

$$a = 2m \sin\left(\frac{2\pi f_m H}{C \cos\psi}\right) .$$

In this equation, H is altitude in km, C is the speed of light in km/s, f_m is the modulation frequency in Hz (either 30,000 or 33,000) and ψ is the angle made by a ray from the antenna to a specific differential surface area with respect to a vertical through the antenna. The value of $J_1^2(a)$ constitutes the specific FM loss associated with each differential area. The power backscattered from each differential area was taken to be proportional to

$$\frac{G_n^2(\theta)\ J_1^2(a)}{\rho^2}\ \Delta\Omega$$

where ρ is the slant range and $\Delta\Omega$ is the differential solid angle; the quantities θ and a were evaluated at each differential area according to its position with respect to the reference vertical passing through the antenna.

The Doppler frequency shift, ν, in the echo from any elementary scattering area is given by the equation

$$\nu = \frac{2V}{\lambda} \cos\gamma ,$$

where γ is the angle between the velocity vector and the line connecting the (center of the) antenna to the (center of the) scattering area. A function proportional to the power spectral density of the echo vs frequency was computed by taking the sum of the terms $G_n^2 J_1^2 \Delta\Omega/\rho^2$ over all differential areas where γ was the same. This computation was carried out separately for each of the two FM rates (30 kHz and 33 kHz) and an average power spectral density found at each Doppler shift frequency.

From the average power spectrum, a quantity proportional to peak power density was determined and the centroid frequency was calculated; this was carried out at a variety of altitudes over the range of interest. (The Venus probe radar instrument would also operate on the average spectrum.) The variation in peak signal density vs altitude is proportional to the variation in S/N ratio vs altitude; the change in centroid position, when normalized by the quantity $2V/\lambda$, indicates the change in calibration constant vs altitude.

For the first of the more exact calculations, horizontal velocity, V_h, was taken to be zero. The resultant variation in S/N with altitude, which appears plotted in Figure 12, clearly shows an altitude hole structure. In this plot, the ordinate scale was determined on the basis that if the ripples in the region from 15 to 35 km were smoothed out, the results would be identical to those which appear in Figure 11 over the same altitude range. Changes in calculated vertical velocity calibration constant, viz. in the quantity $\nu/(2V/\lambda)$, appear in the graph of Figure 13. Smoothing the altitude hole induced ripples out of this last plot would yield a curve which is nearly constant with respect to altitude whose value lies just under $\cos(10°)$.

Next, the more exact calculation was made with horizontal velocity, V_h, taken to be 5m/s, 15m/s and 30m/s, each in turn. In these cases, the total velocity vector is displaced from the vertical spin axis and the angle between the rotating beam and the total velocity vector takes on an oscillatory character. At one extreme the beam is closest to the total velocity vector and the instantaneous Doppler shift is a maximum;

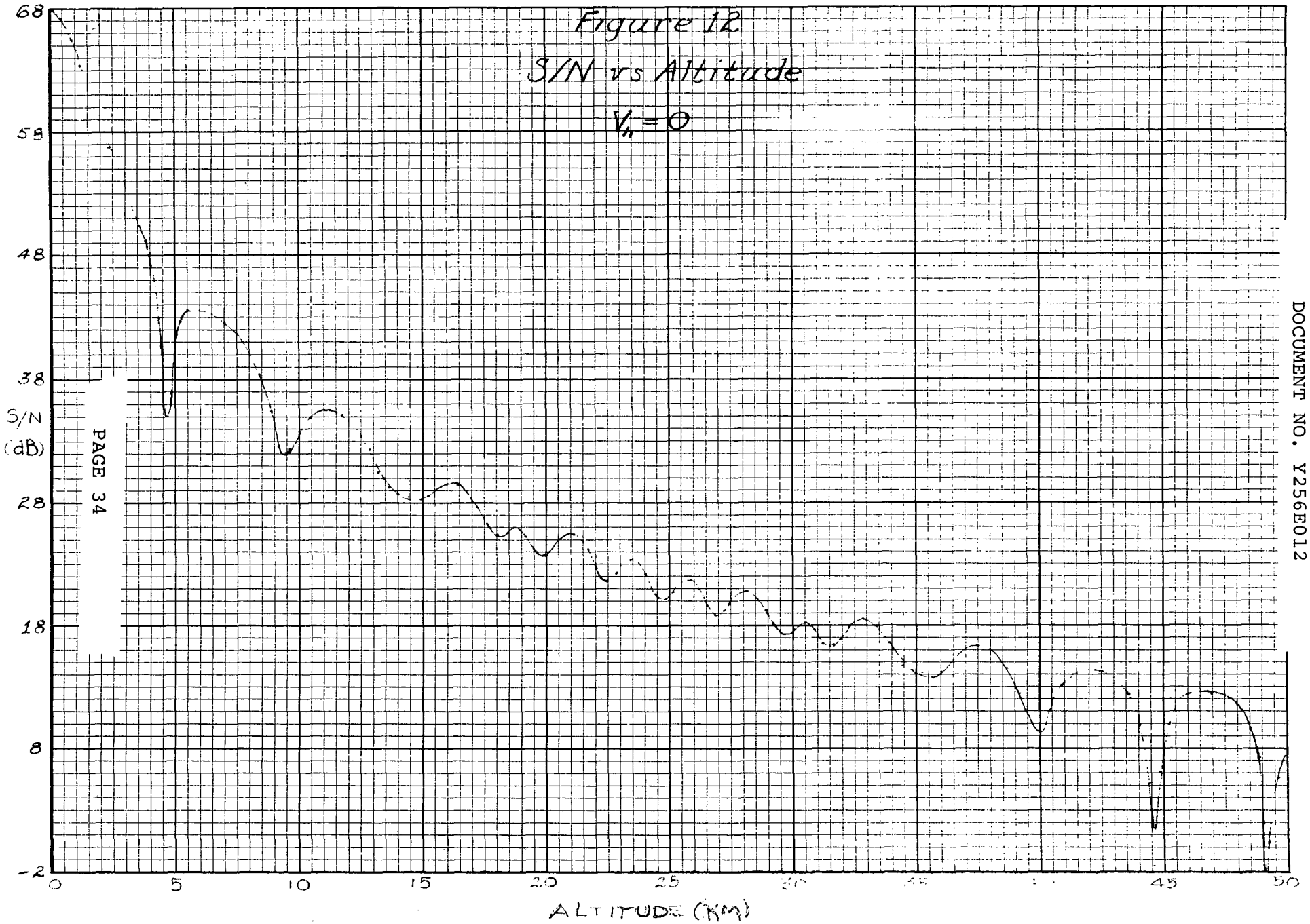

Figure 13

Vertical Velocity Calibration Constant vs Altitude

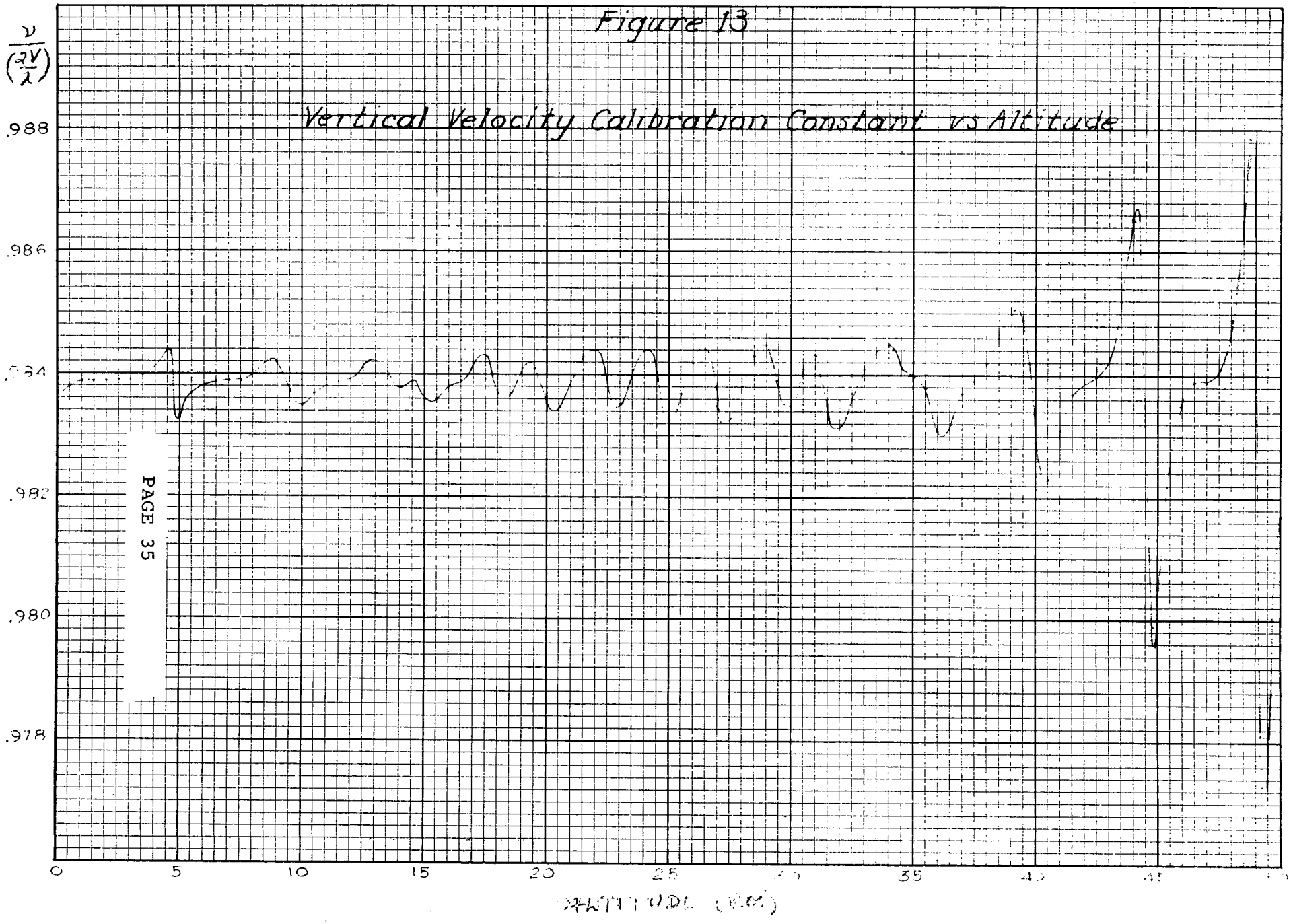

at the other extreme the beam is furthest from the total velocity vector and the instantaneous Doppler shift is a minimum. To keep the volume of computation within reasonable bounds, only the two extremes were examined. Graphs of S/N vs altitude at each extreme are presented in Figures 14, 15 and 16 for V_h = 5m/s, 15m/s and 30m/s respectively. The upper curve in each case corresponds to the maximum shift; the reason for the increase in S/N when going from minimum to maximum Doppler shift is that the echo spectra also become narrower and more peaked. The ordinate scales on these curves were adjusted by comparing the total area under the power spectral density curves (which is proportional to the echo power) in each case at an altitude of 0.1 km. If it is assumed that 30m/s is the maximum horizontal velocity which must be accommodated, then from a S/N point of view, the upper altitude limit for velocity measurement (from Figure 16) should be about 34 km. The possibility exists that the altitude limit may be increased by reducing the response time of the frequency tracker, which is expected to permit tracker operation below a S/N ratio of 6 dB. Further discussion of the considerations affecting the choice of tracker time constant is found toward the end of this section.

Calculation of the vertical and horizontal components of Doppler shift was carried out by means of an abreviated version of the processing scheme intended for the Venus probe radar. (The full procedure is described toward the end of Section 2.2 in connection with the block diagram in Figure 7.) For the purpose of this discussion, let ν_1 be the maximum Doppler shift at a given altitude and let ν_2 be the minimum Doppler shift at the same altitude; then the vertical component of Doppler shift, ν, is calculated from the equation

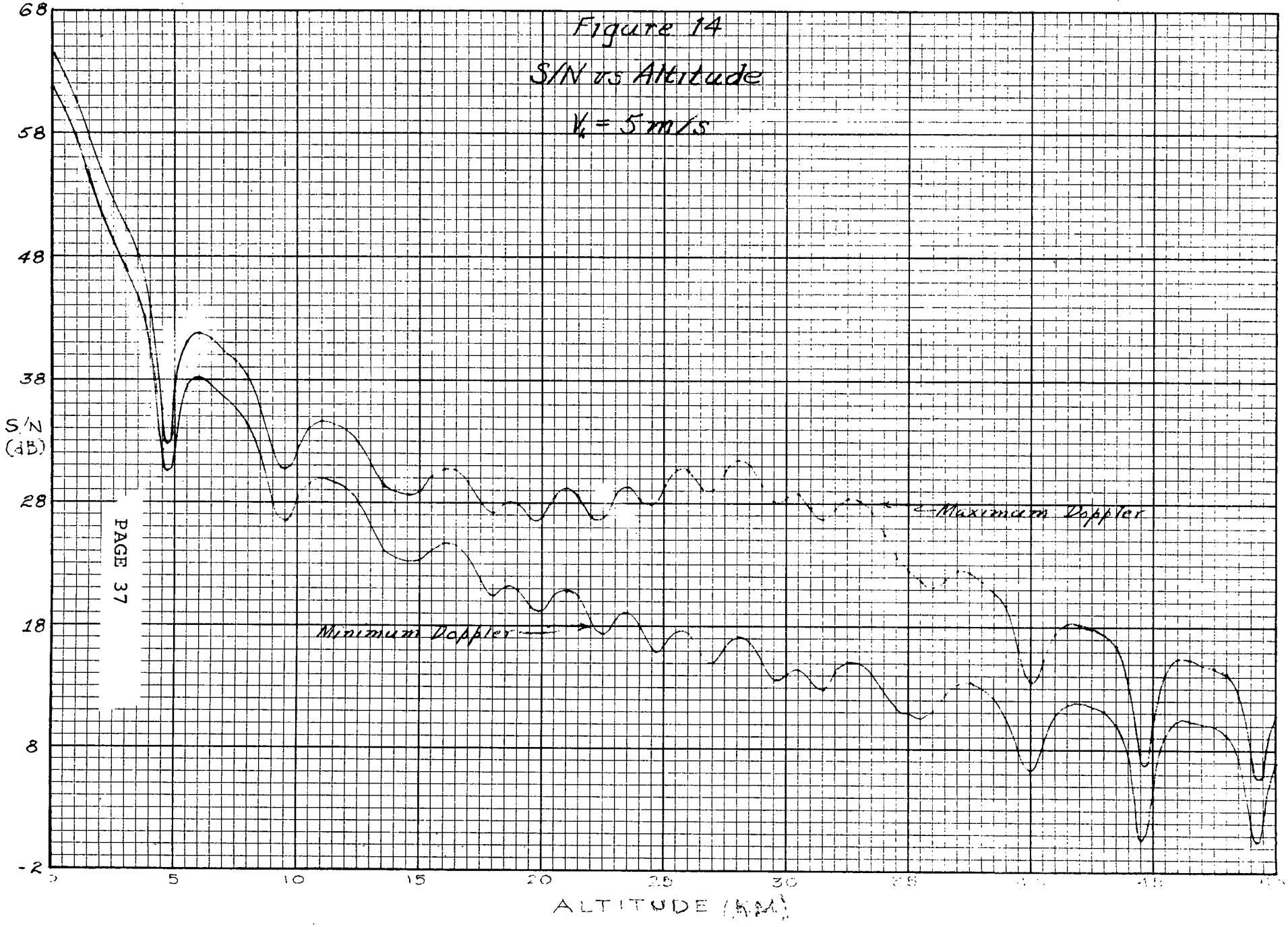

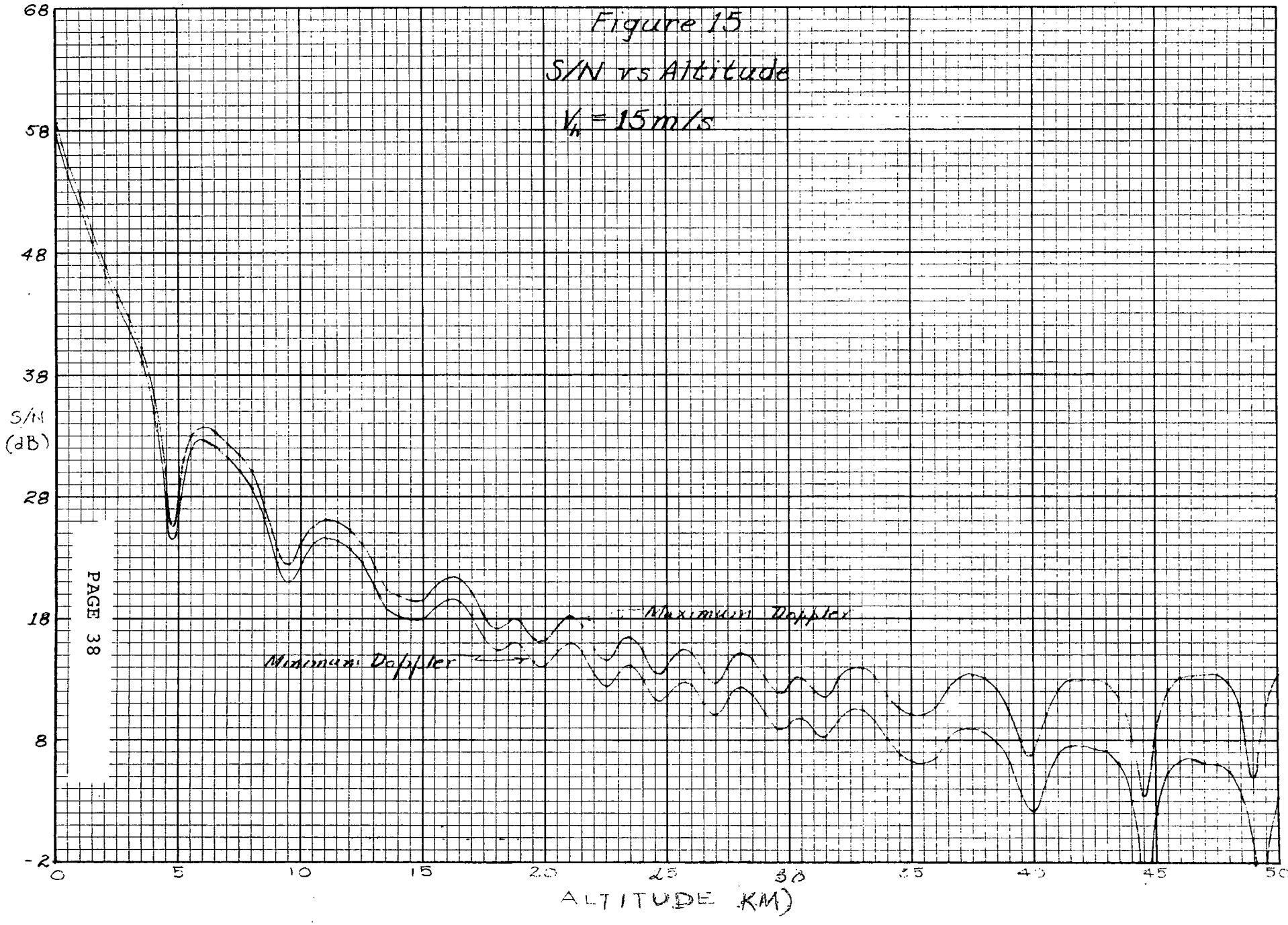

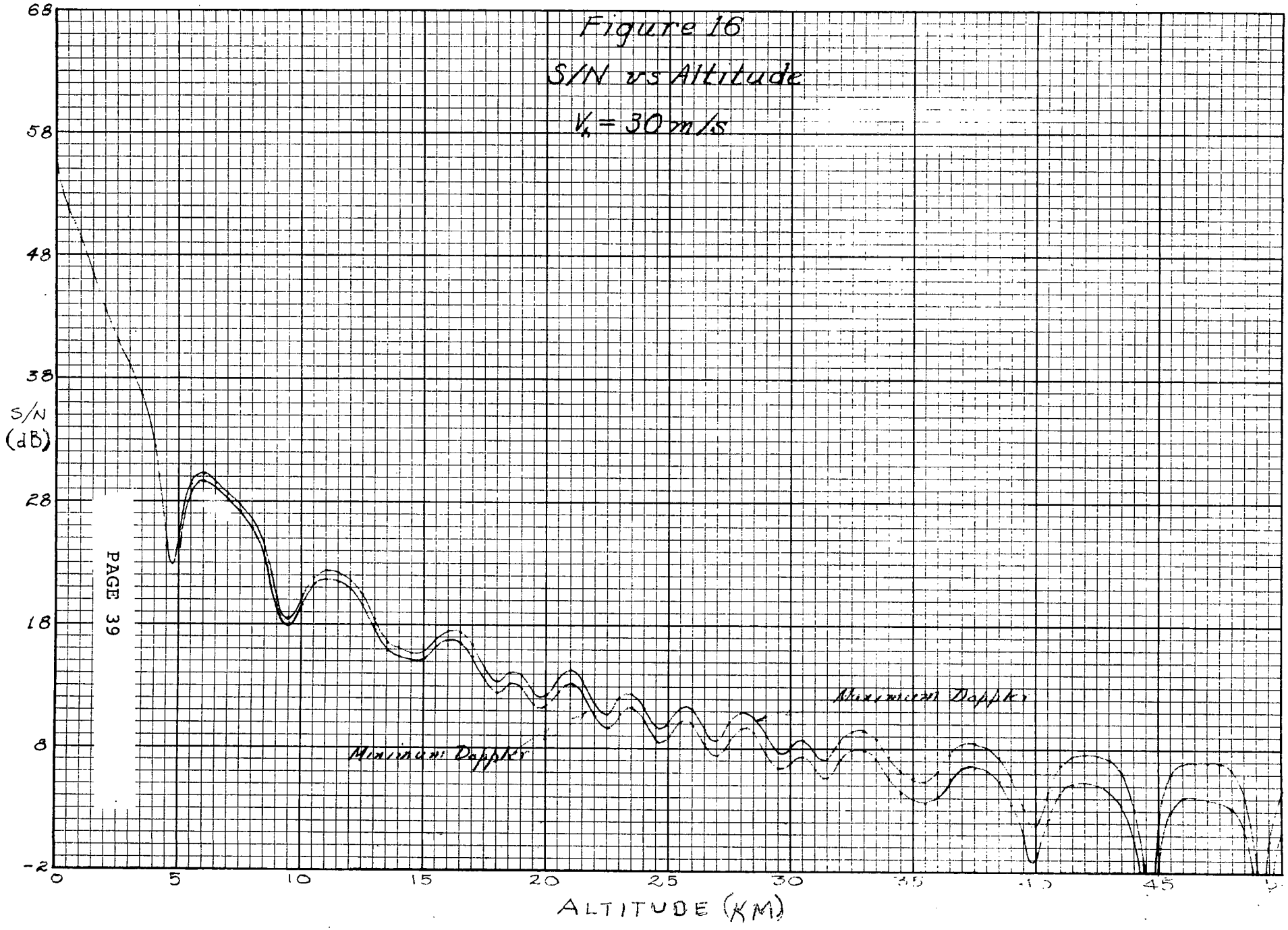

$$\nu = \frac{\nu_1 + \nu_2}{2} \quad ,$$

and the horizontal component of Doppler shift, ν_h, is calculated from the equation

$$\nu_h = \frac{\nu_1 - \nu_2}{2} \quad .$$

When these calculations were carried out and the vertical calibration constant computed from the ratio $\nu/(2V/\lambda)$, V being the vertical component of velocity, the results were virtually identical with those shown in Figure 13, regardless of the value of horizontal velocity assumed. In a similar manner, the horizontal calibration constant was computed from the ratio $\nu_h/(2V_h/\lambda)$; these results, which are presented in Figure 17, were also virtually independent of the value assumed for V_h. With the ripples smoothed out, this last plot would be nearly a constant, independent of altitude, at a value just under sin(10°). The fractional variation of the horizontal calibration constant around its apparent mean at altitudes less than 34 km is less than ±2.4% of the mean while, over the same range of altitude, the vertical calibration constant moves around its mean by less than ±0.08%. Of the two, the change in horizontal calibration constant represents a limitation on achievable precision while the change in vertical calibration constant is clearly negligible.

The maximum altitude at which the altimetry function can be performed is determined by the total signal-to-noise (S_t/N) ratio in the altitude channel just before the doubler. Current experience with the APN-187 altimeter is that S_t/N must be at least 3 dB for the proper operation of the normal phase tracking loops. Reference to the system block diagram of Figure 4 indicates that a double sideband (DSB) Doppler spectrum exists at the output of the altitude post IF whose bandwidth is

controlled by the bandpass filter just preceding the output amplifier. In principle, the width of the bandpass need only be large enough to pass the DSB Doppler spectrum. Assuming this to be the case, the model used to make the altitude hole calculations for the velocity function was extended to calculate S_t/N vs altitude. Two different cases were treated, one being the absence of horizontal velocity and the other being the presence of a horizontal component of 30m/s. For the latter situation, the case of maximum Doppler shift (i.e. radar beam closest to total velocity vector) was assumed. At each altitude, the limiting bandwidth was taken to be 2.5 times the Doppler shift calculated for that altitude (so as to include all of both sidebands). The resultant variation of S_t/N with altitude is summarized by the graphs of Figure 18. Based on a minimum operating value of 3 dB for S_t/N, the curves of Figure 18 indicate an upper limit of 17.5 km for the altitude function. To achieve this performance, the width of the limiting bandpass filter would have to be set at 3750 Hz; with a fixed bandpass, S_t/N would still rise with decreasing altitude, albeit not as rapidly as in Figure 18.

The 3 dB lower limit for S_t/N quoted in the preceding paragraph for the altimeter in a standard APN-187 depends to some extent on the response time of the phase tracking loops. In current versions of the APN-187, the phase loop response time is about 6 ms (based on full time operation of the loop). However, in the Venus probe radar instrument, each normal phase loop would be (alternately) operating for 1/9.6 second, waiting (i.e. opened) for 1/9.6 second and sampled only during the waiting intervals. To permit the loop to do some averaging when it is operating, the loop time constant would be increased to about 60 ms. This, in turn, should permit operation down to a lower value of S_t/N than 3 dB which should result in a somewhat higher

Figure 18

S/N vs Altitude

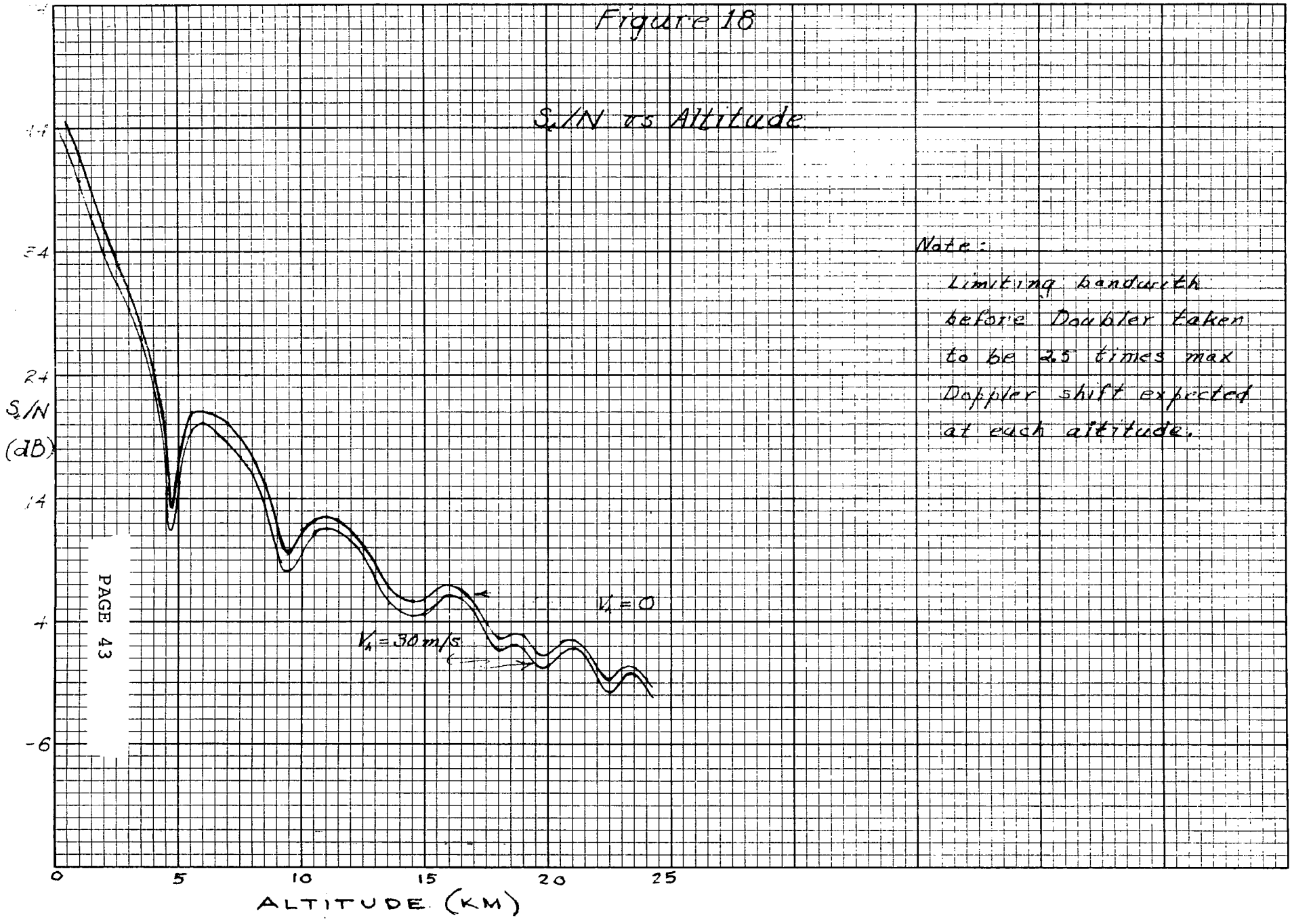

Note:
Limiting bandwith before Doubler taken to be 2.5 times max Dopplver shift expected at each altitude.

limiting altitude for the altimetry function than the 17.5 km figure arrived at on the basis of Figure 18.

A similar situation exists with regard to the altitude limit for the velocity function as a result of an increase in frequency tracker response time appropriate to the Venus probe application. In normal use, the time constant of the SKD-2100 frequency tracker loop would be about 20 ms (based on continuous duty). When used in the Venus probe radar, the frequency tracker output would be sampled at intervals more than 1 second apart. Increasing the frequency tracker response time to about 0.5 second would permit the loop to do some averaging between samples; adjacent samples, however, would still remain statistically independent. As used in the Venus probe radar, the tracker would also be modified to have a second order frequency response. The resultant faster rolloff should attenuate noise that would otherwise be present at odd harmonics of the spin rate; such noise would, if not removed, contaminate the output of the horizontal velocity processors shown in Figure 7 and described in Section 2.2.

The random nature of the backscattering process which produces the radar echo causes the Doppler shifted echo spectrum to have an intrinsic noise-like quality. As a result, the velocity outputs may be expected to fluctuate around their mean values. A worst case situation arises when the probe is near the surface of Venus with a horizontal velocity of 30 m/s and with the beam pointed furthest away from the total velocity vector. The magnitude of the total velocity here is

$$V = \sqrt{10^2 + 30^2} = 31.6 \text{ m/s} \quad ,$$

and the angle between the beam and the total velocity vector is

$$\gamma = \tan^{-1}(3)+10° = 81.6°$$

Taking the one way beamwidth to be 8.1° (from Figure 9) the fractional spectrum bandwidth should be

$$\frac{\Delta\nu}{\nu} = \tan\gamma\ \Delta\gamma \quad ,$$

$$= \tan(81.6°)\times \frac{8.1\pi}{180\sqrt{2}} = 0.676 \quad .$$

At the same time, the Doppler shift frequency should be

$$\nu = \frac{2V}{\lambda}\cos\gamma \quad ,$$

$$= \frac{2\times 31.6}{0.03}\cos(8.16°) = 308 \text{ Hz}$$

If the standard deviation of the instantaneous frequency of the Doppler shifted echo (denoted by σ_ν) were compared to ν, the result would turn out to be about half of the fractional spectrum bandwidth calculated above. Thus

$$\frac{\sigma_\nu}{\nu} \approx \frac{1}{2}\frac{\Delta\nu}{\nu} = 0.426 \quad .$$

The autocorrelation time of the instantaneous frequency fluctuation (denoted by τ_ν) would be given by

$$\tau_\nu \approx \frac{1}{4} \div \frac{\Delta\nu}{2} \quad ,$$

$$\approx \frac{1}{2(0.676)(308)} = 0.00239 \text{ second} \quad .$$

As a result of modifying the frequency tracker to have a 0.5 second response time, the standard deviation of the tracker output fluctuations, σ_t, is reduced and

$$\frac{\sigma_t}{\nu} = \frac{\sigma_\nu}{\nu}\sqrt{\frac{0.00239}{0.5}} \approx 0.0295 .$$

Here it is convenient to decompose ν into the sum of two components, ν_h associated with the horizontal part of velocity, given by

$$\nu_h = -\frac{2V_h}{\lambda}\cos(80°) = -348 \text{ Hz} ,$$

and ν_v associated with the vertical part of velocity, given by

$$\nu_v = \frac{2V_v}{\lambda}\cos(10°) = 656 \text{ Hz.}$$

Since 16 samples are averaged for each vertical velocity output, the relative fluctuation in this quantity is

$$\frac{\sigma_t}{\nu}\cdot\frac{\nu}{\nu_v}\cdot\frac{1}{\sqrt{16}} \approx 0.0295\cdot\frac{308}{656}\cdot\frac{1}{4} = 0.00346;$$

the rms fluctuation error in the vertical velocity output is at most 0.346%. In the case of each horizontal velocity component, the output is the average over 8 samples, giving a relative fluctuation of

$$\frac{\sigma_t}{\nu}\cdot\frac{\nu}{\nu_h}\cdot\frac{1}{\sqrt{8}} \approx 0.0295\cdot\frac{308}{348}\cdot\frac{1}{2\sqrt{2}} = 0.00925 ;$$

the rms fluctuation error in each horizontal velocity output is at most 0.925%.

It is important to note that fluctuations may be expected in the horizontal velocity outputs even in the absence of wind. This is a result of the fact that the same set of samples are processed to derive the vertical and horizontal components of velocity. For example, suppose that there is no wind near the surface, making both the vertical and total velocities 10 m/s. The relative tracker sample fluctuation for this case is

$$\frac{\sigma_t}{\nu} \approx 0.0295 \quad \frac{\tan(10°)}{\tan(8.16°)} \quad \sqrt{\frac{\sin(81.6°)}{\sin(10°)}} \quad ;$$

this result was derived from the one given in the last paragraph by adjusting for the change in γ as it affects both the fractional spectrum bandwidth and the autocorrelation time. The mean Doppler shift, ν, in this case is the same as ν_v in the previous example. After averaging over 8 samples, the resultant horizontal velocity output would be interpreted in real units by dividing with the factor $(2/\lambda)\cos(80°)$. Therefore, the residual fluctuation (rms) in horizontal velocity for this case would be

$$\frac{\sigma_t}{\nu} \cdot \frac{\nu\lambda}{2\cos(80°)} \cdot \frac{1}{\sqrt{8}} \approx 3.69 \quad \frac{cm}{s} \quad .$$

Both of the previous examples were worked out for conditions near the surface of Venus to show worst case situations. Fluctuation errors may be expected to decrease progressively with increasing altitude. As shown in Figure 1, the higher the altitude, the greater the expected velocity. Along with the larger velocity goes a shorter autocorrelation time in the intrinsic data. With a

fixed averaging time, a shorter autocorrelation time means more independent data being averaged and lower fluctuation errors.

2.4 Feasibility Analysis

The predicted operating range and accuracy of the Venus probe radar instrument should be viewed against projected power, weight and size requirements in assessing the feasibility of the conceptual design. Referring to Figure 16 and recalling that a 6 dB value of S/N is needed for reliable operation of the current (fast response) SKD-2100 frequency tracker, it is evident that the maximum altitude for the velocity function should be at least 34 km. Again, recalling that a 3 dB value of S_t/N is required in order that the (short time constant) phase tracking loops of the APN-187 altimeter work properly, it is clear from Figure 18 that the maximum altitude for the altimeter function should be at least 17.5 km. Since this is less than half way up to the common altitude hole for the two FM frequencies to be used, the resultant altitude information should be completely unambiguous.

Over the anticipated operating range for velocity, total errors in the vertical velocity output should be within ±0.9% of the true value. Most of this is caused by variations in the vertical velocity calibration constant which occur at the antenna-atmosphere interface, as shown in Figure 10. Total errors in the horizontal velocity output should be within ±3.0% of the true value over the same operating range. In the case of horizontal velocity, the dominant error source is the variation of the calibration constant caused by altitude hole effects. Reference to Figure 17 shows that the altitude hole structure has a quasi-periodicity. To the extent that wind velocities change with altitude more slowly and with less regularity than the horizontal calibration constant, it may be possible to process the total wind data record (on the ground, after the fact) with

the equivalent of a narrow band elimination filter and reduce the dominant error term.

With regard to the altimeter, current (low altitude) data indicate that the error at each FM frequency should be within ±3% for altitudes up to half the distance to the first altitude hole for that frequency. (At 30 kHz, the first altitude hole occurs at 5.08 km while at 33 kHz, it occurs at 4.62 km.) For still higher altitudes, the error should decrease with altitude until the first hole is reached and then should repeat cyclically between each pair of succeeding altitude holes until the limit of the operating range is reached. Right around the hole altitude for each frequency, a DATA INVALID status signal would be generated for the associated output due to inadequate S_t/N in that channel.

The power requirements of the Venus probe radar were estimated by extrapolating from known power drains in the baseline configuration. Adding together the power used by the stripline front end, the pre IF and post IF modules and the frequency tracker of the SKD-2100 (exclusive of beam switching and time sharing circuitry not needed here) the total of these comes to 12.5 watts. The altimeter circuitry of the APN-187 used here draws 3 watts. Additional circuitry required to mate the altimeter and the modified SKD-2100, and to provide the buffer/interface at the output, is expected to need 8 watts. On top of all this, the use of a transmitting power level of 0.5 watts adds another 25 watts to the power requirements.

The sum of all of the foregoing figures comes to an estimated power drain of 48.5 watts. If all of this power can be supplied directly from the probe batteries at the appropriate voltages (i.e. at +15V, +5V and -15V) then no additional drains need be

provided for. However, if the required voltage levels must be generated in a power conditioner operating off the batteries, then the losses in the conditioner constitute an additional power drain. Assuming an overall efficiency of 70%, which could be achieved by using a more complex (but already available) design to generate +5V in the SKD-2100 power supply, the additional power required comes to 20.8 watts. Under these conditions, the total power required would rise to 69.3 watts.

In a manner similar to that used for the power estimate, projected weights were taken from known module weights. All of the circuitry involved in the velocity function plus the stripline front end, modified timer and output buffer/interface are expected to weigh 2.36 kg (5 lb). The altimeter circuitry plus those modules added to mate the altimeter to the modified SKD-2100 are expected to weigh 0.907 kg (2 lb). The antenna would be a planar array using titanium waveguide with dimensions 1.836 cm x 1.016 cm x 0.0508 cm (0.722" x 0.400" x 0.02"); its weight is expected to be 0.68 kg (1.5 lb). Supplied directly from the probe batteries, the total weight of the radar instrument should be 3.85 kg (8.5 lb). In the event a power conditioner is needed, this would add 3.36 kg (3 lb) to the weight, raising the total to 5.21 kg (11.5 lb).

The space that would have to be allocated within the pressure vessel for all of these components may be estimated on the basis of the current size of the electronics volume of the SKD-2100. The dimensions of this region are 38.1 cm x 38.1 cm x 5.08 cm (15" x 15" x 2") giving rise to a volume of 7380 cm^3 (450 in^3). Allowing additional space for four (4) printed circuit cards with dimensions 7.62 cm x 10.16 cm x 2.54 cm (3" x 4" x 1") adds an additional 787 cm^3 (48 in^3). Considering that at least one item (the antenna switch driver) would be removed from the

SKD-2100 altogether, an overall size estimate of 8200 cm^3 (500 in^3) for the radar electronics seems reasonable.

The planar array antenna would be located outside of the pressure vessel and would occupy a volume with dimensions 25.4 cm x 25.4 cm x 1.905 cm (10" x 10" x 3/4"). Its size is believed to be sufficiently small compared to the 66 cm (26 in) diameter, insulation covered sphere so that it could be faired into the spherical surface without unduly changing the aerodynamic properties of the probe in free fall. A preliminary stress analysis of the waveguide structure showed it to have a safety factor of about 10, considering the stress generated at the weakest parts of the guide (viz. the slots) under conditions of peak deceleration (300 g) and maximum temperature (500°C). It should be noted that detailed design and fabrication procedures for a titanium waveguide antenna will require almost no new development but rather will make use of already well established techniques. (The calculations leading to the size and weight estimates given in the last three paragraphs were made principally using the English system of units.)

Inasmuch as all of the electronic assemblies of the Venus probe radar would be subject only to the controlled environment (i.e. temperature and pressure) inside the pressure vessel, no problem exists in this regard. With respect to the decelerations expected during entry into the Venus atmosphere, it is felt that most of the modules which would be used are already sufficiently rugged from a mechanical standpoint. For those few modules (principally the altimeter elements) which may be mechanically inadequate, a new packaging arrangement would be made. No major impact on either weight or volume is expected to result from such changes.

3. CONCLUSIONS AND RECOMMENDATIONS

On the basis of all of the preceding discussion, it is warranted to assert that the conceptual design of Figure 4 possesses most of the attributes desired in a Venus probe wind/altitude radar. Since the radar instrument would be essentially a modified version of the SKD-2100 joined to the altimeter portion of the APN-187 (both existing equipments) it should be realizable within the constraints of a low cost, minimum development program.

As a means of summarizing the results of this study, a list of output quantities is presented in Table I, with the number of bits assigned to each. Except for the status bits, which show whether the data on the associated channel is valid or not, the number of bits chosen for each quantity is indicative of the limiting accuracy predicted for that quantity. In the case of each horizontal component, an additional bit was allocated to indicate the sign (+ or -) of the component. The allotment of 5 bits to the sample peak timing indicates an expected precision of about ±10° in locating the sampling pulses with respect to the spin cycle.

TABLE I

OUTPUT QUANTITY	No. of Bits
1. Velocity	
a) Vertical Magnitude	7
b) Horizontal Sine Component	6
c) Horizontal Cosine Component	6
d) Status	1
2. Sample Peak Timing (if required)	5
3. Altitude	
a) 30 kHz Phase Angle	5
b) 30 kHz Status	1
c) 33 kHz Phase Angle	5
d) 33 kHz Status	1
TOTAL:	37

One complete data readout (i.e. all 37 bits) would be made for each altitude increment of one kilometer. Since the initial descent rate is about 50 m/s, at the top of the altitude range there would be a complete readout of velocity and altitude approximately every 20 seconds. The average data rate for the radar instrument at high altitudes would therefore be about 2 bits/second.

The parenthetical qualification of item 2 in the table was included to indicate that this output would not be needed if the sampling frequency were locked to the spin rate. Should that situation be achieved (i.e. synchronism between sampling and spin rate) then considerable simplification in interpreting the horizontal velocity outputs. In the event that locked phasing cannot be provided, it would be important to know the spin rate with enough precision so that the sampling frequency could be set within 5% of it.

Another feature of the spin which is important is the orientation of the spin axis. All of the analyses contained in this report assumed that the spin axis would be aligned to the vertical. It is recognized that, in the actual mission, some deviation from the vertical is bound to occur. The effect of such misalignment would be to cross-couple the vertical and horizontal velocity readouts. Since the probe will experience vertical velocity at all times during free fall but horizontal velocity only in the presence of wind, the principal errors introduced by spin axis misalignment would be incurred in the horizontal readouts. In order to keep this error source small compared to those already discussed in Sections 2.3 and 2.4, the deviation of the probe spin axis from the vertical should be kept under 1.5°.

With regard to the not inconsiderable power requirements estimated for the radar instrument, there are two areas where significant savings might be achieved. A cursory examination of the electronics indicates the possibility of reducing the ±15V supply voltages to ±12V with no significant loss in performance. If closer study bears this out, a saving of 4 watts would be gained. The other possibility concerns increasing the efficiency of the Gunn diode RF oscillator; at present, the efficiency at 3 cm is rated at 2%. Since somewhat more than half of the total power required (exclusive of power conditioner) is consumed by the RF oscillator, an improvement of efficiency to just 3% would result in more than 8.5 watts being saved.

Improvement of the efficiency of Gunn diode oscillators is considered well within the realm of possibility by manufacturers of these devices. However, most users are not concerned with the problem (i.e. are not supply power limited) so that the stimulus for research and development in this area is small. It is recommended that NASA sponsor some effort in this area in an attempt to relieve a potential power problem for the Venus probe, either by funding the work directly or by making this an additional Kearfott task under Phase II (to be handled by subcontract).

It is further recommended that NASA authorize Kearfott to proceed with Phase II of this contract. During the next phase critical portions of the conceptual design would be examined in greater detail. Specific circuits would be layed out to perform the new timing functions shown at the lower left in Figure 4 and in the entire diagram of Figure 5. The same course would be followed with respect to the altitude readout scheme of Figure 6 and the velocity readout of Figure 7. Breadboarding and functional checkout of all of these circuit groups would be

undertaken except in the event such a group already exists as an available, operating module on some other equipment. All linear active circuits currently run from ±15V would be tested at ±12V to see if proper operation could be maintained with a consequent saving of power. Likewise, all switching circuits currently used for beam sharing purposes would be studied with a view to possible deletion and a saving of both power and weight. In the case of the antenna, the use of broadwall radiating slots would be considered to implement the configuration shown in Figure 8. Should the use of broadwall slots be possible, then the thickness of the antenna would be reduced to about 1.27 cm (1/2 inch). (This estimate was based principally on the English system of units.) Once the radiating elements have been decided upon, antenna test pieces would be fabricated and then subjected to extensive measurements on an RF range. Using this empirical data, more extensive computer studies of the antenna patterns would be carried out. The scheme for using a leakage signal for altitude calibration purposes would be breadboarded and tested. (It is of interest here that other, in house, Kearfott programs are also planning to use a leakage calibration signal, but with different processing. Any useful results from these efforts would be available to NASA under Phase II.) The need for and effect of blanking between the two different FM intervals would be subjected both to further analysis and to bench tests. In addition to all of the foregoing, any non-qualified items unique to the implementation of the design would be identified. All interface and support requirements associated with the design concept would be worked out in close coordination with NASA Ames.

REFERENCES

[1] Pioneer Venus Baseline System Design, Doc. No. PV-1002-A, P. 5-6, Fig. 5-2.

[2] NASA SP-8011, Models of Venus Atmosphere, Section 2.2.2.5 - P. 26.

[3] Op.Cit. P. 40, Table 5.

[4] "The Lorentz - Lorenz Functions of Argon, Nitrogen and Carbon Dioxide Up to 50 Atmospheres at a Wavelength of 12 mm", by H. W. DeWijn and F. W. Heineken, Physica, 25, 1959, P. 623.

[5] "Laboratory Measurement of Microwave Absorption in Models of the Atmosphere of Venus", by W. Ho and I. A. Kaufman, J. Geophys. Res., 71, Nov. 1, 1966, P. 5102 equation (13).

[6] "Microwave Opacity of Venus Atmosphere", by Duane O. Muhleman, The Astron. J., 74, Feb. 1969, P. 59.

[7] "Propagation of Radio Waves Through the Lower Atmosphere of Venus", by Kurt R. Richter, Rpt, No. X-730-72-323, Goddard Space Flight Ctr., Aug. 1972, P. 17 Fig. 4.

[8] "Radar Studies of Planetary Surfaces", by J. V. Evans, Am. Rev., Astronomy and Astrophysics, 1969, P. 244 Fig. 25.